SPATIAL-TEMPORAL VARIABILITY IN PHYTOPLANKTON BIOMASS AND COMMUNITY COMPOSITION IN TEXAS RESIDENTIAL CANALS

A Thesis

by

JORDANA CUTAJAR

BA, University of Florida, 2017

Submitted in Partial Fulfillment of the Requirements for the Degree of

MASTER OF SCIENCE

in

COASTAL AND MARINE SYSTEM SCIENCE

Texas A&M University-Corpus Christi
Corpus Christi, Texas

August 2022

August 2022

SPATIAL-TEMPORAL VARIABILITY IN PHYTOPLANKTON BIOMASS AND COMMUNITY COMPOSITION IN TEXAS RESIDENTIAL CANALS

A Thesis

by

JORDANA CUTAJAR

This thesis meets the standards for scope and quality of
Texas A&M University-Corpus Christi and is hereby approved.

Michael Wetz, PhD
Chair

Steve Morton, PhD
Committee Member

Jeffrey Turner, PhD
Committee Member

August 2022

ABSTRACT

Harmful algal blooms (HABs) are a natural phenomenon that appear to be increasing worldwide alongside the spread of urbanization and cultural eutrophication. As urbanization increases, many regions around the globe, including Texas, are seeing a significant increase in the number of residential canal systems along their coastlines. These canals pose unique attributes that may enhance conditions for HABs, namely shallow depths, high susceptibility to urban runoff, reduced mixing, and long residence times. Despite this, there has been little research on the water quality and phytoplankton composition of these systems. In this study, water quality and phytoplankton biomass/composition were analyzed in three sites along a mouth-interior gradient of a canal system on Padre Island (Corpus Christi, Texas). It was hypothesized that sites toward the interior of the canal system would experience increased nutrient availability, stratification, phytoplankton biomass/HAB occurrence, and reduced flow. The site at the mouth of the canal system exhibited lower nutrient concentrations and was less susceptible to temporal changes like storm events and stratification than the interior canal sites. Total biovolume did not vary among the three sites; however, phytoplankton composition did. The mouth site was diatom dominant, whereas the interior canals had higher picoplankton biovolumes. Ultimately, this research will (1) assess the water quality along the gradient of the canal system and (2) determine baseline conditions for future monitoring to evaluate shifts in phytoplankton composition and water quality.

DEDICATION

I dedicate this work to all the little girls who dream of becoming scientists. Without the love and support of my parents and friends I never would have donned a white coat or ventured into marine biology. Thank you for believing in me long before I ever did.

ACKNOWLEDGEMENTS

This research would not have been possible without NOAA's Center for Coastal and Marine Ecosystems generous scholarship. I am forever grateful for all the amazing mentorship and educational opportunities awarded to me including scholarships from the Harte Research Institute.

I would like to thank my advisor, Dr. Michael Wetz, and my committee members, Dr. Steve Morton, and Dr. Jeffrey Turner for their guidance. I would also like thank my previous mentor, Alicia McGrew, for her unwavering support over the years. Her encouragement has forever changed the arc of my life.

This project would not have been possible without the support and assistance of my lab mates; Elani Morgan, Molly McBride, Dominic Burch, Laura Beecraft, and Lily Walker. I am grateful for their consistent willingness to lend a hand and learn with me.

Finally, I would like to thank the community of graduate students I was lucky enough to learn from and befriend during my time in Texas. Alexis Neffinger, Molly McBride, Monisha Sulga, Alyssa Outhwaite, and Robert Mueller became my family and even made Texas home. I feel I have grown to become a better scientist and person because of them. I would not have made it through the last two and a half years without their strength, kindness, knowledge, and laughter. Thank you for everything.

TABLE OF CONTENTS

Page

LIST OF FIGURES

Page

LIST OF TABLES

Page

CHAPTER I: INTRODUCTION

Harmful algal blooms (HABs) appear to be increasing worldwide alongside the spread of urbanization and cultural eutrophication (Anderson et al., 2002; Cloern, 2001; Glibert & Burkholder, 2006). As a result, HABs are being documented in locations with no history of HAB activity, presenting new environmental and human health challenges (Verity, 2010). Coastal regions, in particular, are becoming more vulnerable to HABs, as they boast high rates of urbanization and population growth that lead to increased nutrient loads and altered hydrology (Bricker et al., 2008; Neumann et al., 2015). In the Gulf of Mexico alone, the population of coastal communities increased by 150% from 1960-2008 (Wilson & Fischetti, 2010). Other coastal regions in the United States are also becoming more populous, with 29% of the total population residing in coastal counties (Wilson & Fischetti, 2010).

As coastal zones become more populated, estuarine systems have increasingly been modified by the creation of waterfront properties with canal systems (Dellapenna et al., 2015). Approximately 77 percent of the total global length of artificial residential waterways can be found in North America. These canals are unique in their design, which favors longer, narrower systems and more dead ends than canals on other continents (Waltham & Connolly, 2011). Despite the prevalence of canals, there has been limited research on the water quality and phytoplankton composition of these systems. In brackish retention ponds, which are similar to canals in their aesthetic goals, artificial design, and proximity to urban areas, restricted flow combined with nonpoint source pollutants like fertilizer, pesticides, and reclaimed water all contribute to eutrophication and increased prevalence of HABs (Lewitus et al., 2003, 2008). Residential canals tend to be situated in developed areas where they are susceptible to urban runoff and associated nutrient pollution. The increasing use of land-based fertilizer has been

attributed to nutrient loading in neighboring water bodies via runoff (Anderson et al., 2002; Lewitus et al., 2003, Ivey et al., 2020). Cultural eutrophication has been cited as a driving factor for the spread of HABs, which are often correlated with increased nutrients, particularly NH_4^+ and organic nutrients (Anderson et al. 2002, Verity, 2010). Another important feature of many residential canals is that they are shallow, which may facilitate exchange between the water column and sediment in terms of nutrients and gases such as oxygen (Nixon, 1988). For example, nutrient exchange tends to be greater in shallower water bodies, which are more likely to have higher rates of primary productivity as a result (Boynton et al., 2018). However, this exchange can be modulated by stratification (Baustian et al., 2014). In estuaries, hypoxic conditions tend to be most pronounced during stratification (Cloern, 2001). During hypoxia, ammonium and other nutrients may build up in bottom waters and eventually become available to phytoplankton via diffusion through the pycnocline or following the breakdown of stratification (Kemp, 1990). A stratified system can also create an opportunistic habitat for dinoflagellates that are able to migrate throughout the pycnocline and utilize regenerated nutrients, in contrast to non-swimming phytoplankton like diatoms (Paerl et al., 1988 Paerl et al., 2010, Paerl et al., 2014). Finally, it is likely that canals have restricted flushing rates, depending on their design. Generally, high flushing rates can often reduce the effects of eutrophication (Dillon, 1975), whereas slower flushing rates have been associated with increased phytoplankton biomass and the proliferation of HABs, especially in shallow systems susceptible to nutrient loading (Boynton et al., 2018). Reduced flushing may also favor slower-growing dinoflagellates which typically require water column stability to bloom (Paerl, 1988).

As coastal populations increase, canal communities are likely to become more prevalent to accommodate community needs. Because these canals have attributes that may facilitate water

quality degradation and HABs, there is a need to better understand the ecology of these manmade systems as a first step towards developing management actions. In this study, the water quality and propensity for HAB formation were studied along an interior- to-mouth continuum of a residential canal system. The goal of this study was to assess the water quality and phytoplankton composition in a residential canal system on the rapidly developing North Padre Island Canal (Corpus Christi, Texas). This study tested the hypothesis that nutrient availability and stratification will increase/intensify at sites closer to the interior of the canal system, which will lead to increased phytoplankton biomass and the occurrence of HABs. Results from this study can inform community members, water resource managers, and coastal developers looking to foster healthy water bodies in urban areas.

CHAPTER II: METHODS

Site characteristics

The residential canal system in this study is located in North Padre Island, Corpus Christi, Texas (Fig. 1). Site 1 is situated at the mouth of the canal system and is adjacent to the Upper Laguna Madre. Sites 2 and 3 are in the interior of the canal system and were selected to represent more developed residential canals. Site 2 is located approximately 6.43 kilometers from the mouth of the canal system, with homes on one side of the canal. Site 3 is located approximately 3.22 kilometers from the mouth of the canal system and is surrounded by homes on either side.

Sample collection and processing

All sites were sampled on a biweekly to monthly basis to evaluate environmental conditions and phytoplankton composition in the canal system. During the fall and winter, samples were collected once a month, while in the spring and summer seasons, sampling switched to bimonthly. There were 19 total sampling trips from November 2020 until October 2021.

At each sampling location, acid-washed brown 1 L HDPE bottles were used to collect water samples at the surface of the water body. Water samples were immediately stored on ice for transport. Hydrographic data (dissolved oxygen, pH, conductivity, salinity, and temperature) was collected at each sampling location at 0.5 m intervals in the water column using a YSI multiparameter sonde. Stratification strength was estimated by subtracting salinity recorded at the bottom of the water column from salinity recorded at the top. Precipitation data was gathered from the National Oceanic and Atmospheric Administration's National Weather Service and represented a cumulation of 7 days prior to the sampling date. A Secchi disk was deployed at each site to determine water clarity. Field conditions, including temperature, wind speed, and

weather were also recorded. An additional water sample was taken at the surface for phytoplankton analysis in acid washed 500 mL brown HDPE bottles. These samples were stored at ambient temperature.

Once at the lab, water samples were filtered through precombusted 25 mm GF/F filters. Filtrate was frozen and later analyzed for inorganic nutrients. The following nutrients were analyzed: nitrate, nitrite, ammonium, orthophosphate and silicate. 25 mL of water was filtered through Whatman GF/F filters for chlorophyll *a* analysis. Samples were analyzed using 90% acetone and a Turner fluorometer. Water collected for inorganic nutrients (ammonium, nitrite, nitrate + nitrite, and orthophosphate) were filtered through 25 mm GF/F filters and frozen at -20 ºC until analysis. Once samples were ready for nutrient analysis, they were thawed to room temperature and analyzed using a Seal QuAAtro autoanalyzer. Ambient water samples collected for phytoplankton enumeration were stored in amber glass bottles and acidified using Lugol's solution (ratio 60 mL water to 1 mL: Lugol's). An inverted microscope and Utermöhl setting chambers were used for phytoplankton identification and enumeration (Utermöhl, 1931, Utermöhl, 1958). 4-10 ml of sample was settled in chambers for 24 hours. Phytoplankton were counted using an Olympus 1X-71 inverted microscope. Counts persisted until at least 100 cells of the most abundant genera were identified. The volume settled and the area of the chamber were used to calculate abundance of each taxa identified. Each taxon was then classified by shape using Hillebrand et al. (1999) and Sun and Liu (2003) to calculate biovolume (Appendix A). Picoplankton abundance and biomass were estimated using a BD Accuri C6 Plus Flow Cytometer. Samples were preserved using 80 µl of glutaraldehyde mixed with 4 mL of sample water and stored at -80˚C until time of analysis. Samples were then thawed in total darkness and filtered through 20 µm Nytex mesh before being analyzed on the flow cytometer.

A subset of samples was selected for Scanning Electron Microscopy (SEM) to identify potentially harmful genera down to the species level using a Jeol JSM-IT200 InTouchScope. 1-8 mL of the Lugol's preserved samples were filtered and then rinsed with 10 mL of decreasing concentrations of filtered seawater until reaching the final rinse done with freshwater. The filter was then rinsed with increasing 10 mL concentrations of ethanol until a final rinse of 100 % Ethanol was completed. The filter was added to a Denton Vacuum, Desk V model Sputter Coater equipped with a Gold/Palladium (Au/Pd) target, before being transferred to the SEM for analysis.

Statistical analyses

A Principal Component Analysis (PCA) was created in PRIMER v7.0.13. to visualize variability of temporal and nutrient parameters based on site and season. Non-metric multi-dimensional scaling analyses (nMDS) using Bray-Curtis similarity matrices were used to characterize phytoplankton biomass. Since most of the environmental and phytoplankton data collected did not have a normal distribution, a log transformation was applied prior to running statistical analyses in Primer.

Data were also analyzed using R-Studio. Since data were non-normal, untransformed values were analyzed using Kruskal-Wallis one way analysis of variance to determine if there were significant differences in environmental and phytoplankton parameters based on site and season. Spearman's rho correlations were used to determine the relationship between phytoplankton parameters and environmental data.

CHAPTER III: RESULTS

Environmental conditions and variability

There were no significant differences in temperature among the three sites ($p=0.81$); however, there were significant differences in temperature based on season ($p<0.01$). The lowest temperatures were recorded in February 2021 following a freeze event, while the highest temperatures were in August (Fig. 2). Salinity was another parameter that did not have significant differences based on site ($p=0.40$). Higher salinity was observed in the winter and spring, while the lowest salinity generally occurred during the summer (Fig. 3). Following a rain event in early July, sites 2 and 3 experienced their lowest recorded salinities; 5.1 and 14.9, respectively (Fig. 3), whereas site 1's lowest recorded salinity, 20.3, occurred later that month. The only instances of stratification documented throughout the study occurred following heavy rainfall events, particularly in the beginning of May and July. The intensity of stratification varied based on site. Generally, site 1 experienced little to no stratification (Fig. 4). The rain events created the greatest instances of stratification for site 2 (Fig. 5). The highest stratification strength recorded, 17, occurred in early May for site 2. During this time site 3's stratification strength was 8. Rainfall in July also produced instances of stratification for the interior canals, but not the mouth.

pH was not significantly different among the three sites ($p=0.07$); however, sites 1 and 2 experienced reduced pH's (7.04, 7.02) in the beginning of May 2021 coinciding with decreased salinity (Fig. 4). There were significant differences in Secchi depth between sites 1 and 3 and sites 2 and 3 ($p<0.01$), with site 3 experiencing greater Secchi depths than the other sites (Table 2). Secchi was deeper (increased clarity) for all three sites when sampling first began in November 2020; however, depths decreased (reduced clarity) in the winter. Secchi depths

increased again in the spring (Fig. 8). In the summer, Secchi depths varied among the three sites with site 1 experiencing an increase in June, site 2 decreasing, and site 3 increasing in July. However, all three sites began experiencing deeper Secchi readings again in fall, a period of increased salinity and reduced rainfall (Fig. 8).

Surface dissolved oxygen (D.O.) also varied among the sites. There were significant differences ($p=0.02$) between sites 1 and 2, with site 1 experiencing higher D.O. on average. The highest D.O. was recorded in February, following the freeze event (Fig. 9). During this time, D.O. rose to 7.99 mg/L for site 1, 8.08 mg/L for site 2, and 11.02 mg/L for site 3. By March, D.O. had decreased for all three sites, however, sites 2 and 3 experienced lower D.O. than site 1. In the beginning of spring, D.O. began to increase again for all three sites. Site 1 continued to ascend with minor decreases in early summer, but sites 2 and 3 experienced reductions in D.O. during this time. In the beginning of September, sites 1 and 2 experienced their lowest D.O., 2.82 mg/L and 3.7 mg/L respectively, while D.O. at site 3 was increasing. For the rest of sampling, D.O. continued to increase for all three sites. Generally, bottom D.O. was less than surface D.O., excluding three instances for site 1 (February, April, and October 2021) in which bottom D.O. was slightly higher than surface D.O. For sites 2 and 3 bottom D.O. was always less than surface D.O. Hypoxic conditions (D.O. < 2.0 mg/L) were generally recorded at the bottom of the water column at site 2; although, site 3 also had instances of hypoxia in April and again in mid-August 2021 (Figs. 11 & 12). While site 1 did not experience hypoxic conditions, site 2 experienced hypoxia in March, May, and July-October of 2021 (Figs. 10 & 13).

In regard to the nutrient parameters, sites 2 and 3 experienced higher averages of orthophosphate than site 1 (Table 2). Sites 2 and 3 mirrored each other with peaks in March, May, and July (Fig. 13). Site 2 experienced the highest orthophosphate values of all the sites,

15.1 µM, in May and 16.4 µM in July (Fig. 13). During this time, site 3 also experienced an increase in orthophosphate values, reaching 10.1 µM in May and 8.2 µM in July. Site 1 did not experience elevated orthophosphate at any point during the study; orthophosphate averaged less than 1 µM for the duration of the study (Table 2). Orthophosphate was not correlated with temperature ($p=0.17$) or salinity ($p=0.14$).

Site 1 experienced significantly lower nitrate + nitrite (N+N) than sites 2 and 3 ($p <0.01$). When sampling began in November 2020, sites 2 (7.2 µM) and 3 (5.4 µM) were experiencing moderately high N+N. Similar N+N was reported for site 2 and 3 in December before decreasing to low levels as seen at site 1 in January (<1.0 µM). However, following the freeze event in February 2021, N+N started increasing for sites 2 (8.3 µM) and 3 (1.2 µM), with site 3 continuing to increase in March (4.1 µM). Sites 2 and 3 experienced elevated N+N levels following rain events in May (Site 2= 12.5 µM, Site 3=10.1 µM) and July (Site 2=8.21 µM, Site 3=8.17 µM) (Fig. 14). N+N was highly variable throughout summer, and generally lower in fall than at other times. Overall, N+N was not correlated with salinity ($p= 0.44$) or temperature ($p=0.17$).

On average, site 1 experienced the lowest ammonium levels, followed by site 3 and site 2 (Table 2). However, there was no significant difference between sites owing to pronounced variability. Prior to a freeze event in February, ammonium was low at all three sites in December and January (Fig. 15). Following the freeze, site 2 experienced the highest recorded ammonium level (25.1 µM). During this time, site 3 experienced the second highest ammonium level (17.8 µM) in March, which then decreased in April. All three sites experienced increased ammonium in May, before falling and slightly increasing again in July and August. There was no relationship between ammonium and temperature ($p=0.14$). A negative correlation between

ammonium and salinity was observed for site 1 ($p=0.05$), but there was no correlation between ammonium and salinity for sites 2 and 3.

Site 1 experienced the lowest average silicate values throughout the study, followed by site 3, and then site 2 (Table 2). All three sites experienced relatively low silicate in the fall and winter of 2020 (Fig. 16). In spring, silicate levels began increasing for all three sites, and site 2 reached the highest recorded silicate value of 242 µM in May. Silicate also increased in the spring for sites 1 and 3, followed by slight decreases towards the end of May and a renewed increase in July before dropping off again. All sites experienced elevated silicate values in July 2021, with sites 1 and 3 experiencing their highest recorded silicate values of 106 µM and 125 µM during this time. By August, sites 2 and 3 were experiencing decreases in silicate, but site 1 only decreased slightly. Silicate values for all three sites began decreasing in the fall, with a similar trend occurring in the winter. Silicate values were negatively correlated with salinity ($p<0.01$) but positively correlated with temperature ($p<0.01$).

Dissolved inorganic nitrogen to silicate (DIN:Si) ratios were typically low for all three sites (<0.30), suggesting nitrogen limitation. DIN:Si ratios increased in March 2021, with site 3 experiencing the highest recorded ratio of 1.10 and site 2 reaching 0.64 (Fig. 17). Dissolved inorganic nitrogen to orthophosphate (DIN:PO4) ratios were significantly different between sites 1 and 2 (Table 2). Site 2 experienced the lowest average DIN:PO4 ratios throughout the study (8.09), followed by site 3 (28.4) and site 1 (42.1). There were four major increases in DIN:PO4 occurring in February, May and June, then August in which sites 1 and 3 surpassed the 16:1 Redfield ratio indicating phosphorus limitation (Fig. 18).

From the Principal Component Analysis (PCA), PC1 accounted for 36.7% of the variation and PC2 accounted for 23.0% of the variation, resulting in a combined total of 59.7%

(Figs. 16 & 17). The PCA illustrates that site 1 generally experienced lower nutrient and chlorophyll than sites 2 and 3. The PCA also revealed a separation of environmental conditions in winter months from the other seasons, with higher D.O. during that time, and generally higher nutrient variability (PC1) in spring-summer than fall-winter (Fig. 19).

Phytoplankton dynamics

Site 1 had consistently lower chlorophyll *a* with values under 15 µg L^{-1} ($p=<0.01$) throughout the study. In January 2021, site 2 experienced its highest recorded chlorophyll *a* value, 43 µg L^{-1}. Interestingly, site 3 experienced lower chlorophyll *a* during this time but experienced a peak of 45 µg L^{-1} in February. While site 3 increased in February, site 2's chlorophyll *a* decreased. During this time, site 1 experienced its highest recorded chlorophyll *a* of 14.7 µg L^{-1}. Sites 2 and 3 experienced their second highest recorded chlorophyll *a* during June 2021 (Fig. 21). No relationship was observed between chlorophyll *a* and salinity ($p=0.34$) or temperature ($p=0.68$) for the three sites. However, chlorophyll *a* was positively correlated with orthophosphate, N+N, silicate and DIN:Si (Table 2).

There were no significant differences between the sites ($p=0.68$) or seasons ($p=0.42$) based on total biovolume. All three sites experienced similar increases in total biovolume in February, which then decreased in March (Fig. 22). Total biovolumes started increasing slightly in April for sites 2 and 3, and site 1 experienced its highest recorded total biovolume (1.1×10^7 $\mu m^3/ml$). Total biovolumes decreased again for all sites in the following month before rising again in June. Site 3 experienced the highest recorded total biovolume of all three sites during this time at 1.6×10^7 $\mu m^3/ml$. Total biovolume decreased again for all three sites in July before increasing in August. By the end of August, the interior canal sites were experiencing decreased total biovolume, while site 1 experienced a slight increase in total biovolume. All three sites

continued to experience decreasing total biovolumes in September before starting to rebound in October. Despite total biovolume readings not always matching up with increases and decreases in chlorophyll *a*, both were positively correlated ($p<0.01$). Total biovolume was negatively correlated with orthophosphate levels ($p=0.02$) but showed no correlation with other environmental parameters.

There were significant differences in diatoms and picoeukaryote biovolumes, with site 1 having higher diatom biovolumes and lower picoeukaryote biovolumes when compared to sites 2 and 3. Site 3 experienced significantly higher biovolumes of Euglenoids than site 1 ($p<0.01$). On average, diatoms were the greatest contributors to total biovolume for site 1 (63.7%), followed by cyanobacteria (29.8%), and dinoflagellates (17.3%). Every other group examined contributed less than 10% to the average total biovolume (Fig. 23). Picoeukaryotes made up 37.9% of site 2's average total biovolume, more than 4 times the contribution of picoeukaryotes at site 1. Diatoms were, on average, the second greatest contributor to site 2 average biovolume (26.2%). Dinoflagellates (13.3%) and picocyanobacteria (10.8%) made similar contributions to site 2's total biovolume (Fig. 24). Dinoflagellates (26.2%), picoeukaryotes (25.8%), and diatoms (23.5%) were the three highest contributors to average total biovolume for site 3 and together made up over 75% of the total biovolume (Fig. 25). Picocyanobacteria (12.0%) was the fourth largest contributor to the average total biovolume for site 3.

Diatoms made up the greatest percent contributions to total biovolume at site 1 except on December 11th, 2020, March 17th, 2021, April 19th, 2021, August 17th, 2021, and September 3rd, 2021 (Fig. 26). In December and March cryptophytes made significant contributions to total biovolume. In the beginning of April diatoms returned as the dominant group, but that was short lived. While diatoms still made up a significant proportion of the total biovolume on April 19th,

2021, cyanobacteria became the dominant group due to *Trichodesmium* sp. *Trichodesmium* was only observed during this one sampling event and was not detected in the other sites; however, this one appearance made cyanobacteria the second greatest contributor to the average percent contribution to total biovolume for site 1 (Fig. 23). On August 17th, 2021, the dominant group shifted again, this time to dinoflagellates. During this sampling, dinoflagellates included, *Akashiwo sanguinea*, *Cochlodinium sp., Gyrodinium sp.*, *Oxyphysis sp.*, and *Scrippsiella sp*. However, *Cochlodinium sp.* contributed the most to biovolume for the dinoflagellate group during that time (data not shown). Diatoms returned to contributing to the bulk of total biovolume in the fall, but dinoflagellates remained the second greatest contributor to total biovolume until October when picoplankton abundances increased.

Picoeukaryotes and diatoms were the main contributors to total biovolume for site 2 on average, but in January dinoflagellates made up the greatest contribution to total biovolume (Fig. 27). Cryptophytes closely matched dinoflagellates in terms of percent contribution during this time and were a dominant group in the fall and early winter. In February, site 2's elevated total biovolume was mostly attributed to diatoms, as had also been the case for site 1 during this time. In the spring, site 2's total biovolume transitioned from diatoms and dinoflagellates to predominately picoeukaryotes (Fig. 28). Following rain events in July, site 2 saw an increase in chlorophytes which contributed to almost 50% of the total contribution to total biovolume during this period (Fig. 29). In August diatoms increased in biovolume while in fall, picoeukaryotes made a sizeable contribution to total biovolume, along with diatoms and dinoflagellates. Chlorophytes also remerged in October following rain events.

For site 3, cryptophytes were the dominant group in December followed by an increase in dinoflagellates in January (Fig. 30). Similar to sites 1 and 2, site 3 experienced a shift to diatoms

in February following the freeze event. The elevated diatom biovolumes experienced by all three sites in February were characterized by a variety of diatoms, but *Chaetoceros* sp. made up the greatest contribution for all sites (Data not shown). During the rainy spring season, picoplankton were the main contributors to total biovolume. In June when precipitation rates decreased and salinity rebounded, site 3 experienced it's highest recorded total biovolume due to Euglenoids, which contributed to more than 75% of the total biovolume for that period (Fig. 31). Dinoflagellate abundances also increased during this time and were mainly composed of *Gyrodinium sp.* and *Protoperidinium sp*. Biovolume decreased in July but increased again in early August and was characterized by diatoms, including *Chaetoceros sp.*, *Thalassionema sp.*, and *Cylindrotheca sp*. By the end of August, the composition shifted to dinoflagellates like *Cochlodinium sp.*, *Akashiwo sanguinea*, and *Scrippsiella sp.* (Table 3). While total biovolume did decrease in September, the dominant group remained dinoflagellates with *Cochlodinium sp.*, *Prorocentrum sp.*, and *Scrippsiella sp.* among the greatest contributors to total biovolume. For the remainder of the fall season, dinoflagellates, picoplankton, and diatoms were the three greatest contributors to total biovolume.

Diatoms were negatively correlated with N+N, orthophosphate, and silicate, and positively correlated with DIN:PO4 and D.O. (Table 2). The only significant correlation observed for dinoflagellates was a positive correlation with Secchi depth (Table 2). Both picoeukaryotes and picocyanobacteria were negatively correlated with ammonium, DIN:Si and D.O., and positively correlated with silicate and temperature (Table 2). Additionally, picoeukaryotes were negatively correlated with DIN:PO4 (Table 2). Euglenoids were positively correlated with ammonium and N+N (Table 2).

CHAPTER IV: DISCUSSION

Residential canals are expanding worldwide, but little is known about the water quality of canals or their susceptibility to degradation resulting from the extensive urbanization around them. Because canals tend to be shallow, likely not well flushed, and susceptible to urban runoff, there is a possibility for nutrient enrichment and symptoms such as HAB formation, among others. Therefore, it is critical to quantify environmental conditions in canals and to identify drivers of poor water quality for effective long-term monitoring and management of these resources. In this study, water quality conditions were assessed over the course of one year at three sites representing a gradient within the Padre Island canal system, with a goal of quantifying spatial-temporal distribution of nutrients, phytoplankton biomass and composition. During the sampling period, the region experienced a typical seasonal temperature cycle, wet and dry conditions, and extreme weather phenomena including a freeze and heavy rainfall events. It was hypothesized that nutrients and phytoplankton biomass would increase further away from the mouth of the canal system, but this hypothesis was only partially confirmed, as discussed below.

In this study, the interior canals (sites 2 and 3) generally had higher nutrient (orthophosphate, N+N, silicate) concentrations than the mouth of the canal (site 1). Other studies of bay systems and associated canals have reported similar patterns of increased nutrients near canal structures (Corliss & Trent, 1971), especially in the wake of storm events (Wachnicka et al., 2020). Despite the mouth site experiencing significantly lower nutrients than the interior canals, total phytoplankton biovolume did not vary significantly among the three sites. However, chlorophyll *a* was higher in the canal sites, a finding that has been noted in other studies comparing canal systems to their associated coastal bays (Maxted et al., 1997). The discrepancy

between total biovolume and chlorophyll *a* could be due to several factors. Previous research has shown that limited light availability can result in the increase of pigment production in a cell (Falkowski, 1980, Lewitus et al., 2005) Studies have also found that variations in nutrients, and species composition can impact the amount of chlorophyll *a* per cell (Chan, 1980, Lewitus et al., 2005). Likewise, variations in cell structure have also been cited for differences in carbon to chlorophyll *a* ratios and biomass between different groups of phytoplankton (Chan, 1980). Additionally, large central vacuoles, commonly found in centric diatoms, can contribute to lower biomass to volume ratios (Chan, 1980). In all three sites, especially site 1, diatoms were important contributors to total biovolumes, which was not always reflected in chlorophyll *a*.

Phytoplankton community composition varied from the mouth to the interior sites, with site 1 being characterized by diatoms, as is common in estuaries (Cloern, 2018), while the interior canal sites experienced higher contributions from picoplankton. Intense changes in the physical environment coupled with continuous mixing of the water column is known to favor diatoms over picocyanobacteria which often make use of regenerated nutrient sources (Ning et al., 2000). Site 1's phytoplankton composition was also similar to nearby Corpus Christi Bay, a shallow, wind-driven system, which is also dominated by diatoms (Flint, 1984). While diatoms were still a dominant group in the interior canals, their contributions were often overshadowed by picoplankton, particularly picoeukaryotes. While picoplankton have often been associated with low nutrient environments, like the open ocean (Cloern, 2018), recent studies have begun documenting their presence and even proliferation in high nutrient estuarine systems (Gaulke et al., 2010; Mitbavkar et al., 2012; Murrell & Lores, 2004; Pulina et al., 2017). Reduced vertical mixing and flushing in the interior canal sites may be a crucial component to distinguishing between the dominant phytoplankton groups observed throughout the Padre Island canal system.

Although flushing rates were not directly measured in this study, it has been theorized that canals tend to experience reduced mixing, partly due to wind shielding caused by buildings in urban areas (Corliss & Trent, 1971; Xing et al., 2018). Studies of picoplankton in the Baltic Sea found that picocyanobacterial abundances were greatly reduced with increased mixing (Kuosa, 1991) while studies of lagoons and bays in Florida (USA) have linked the proliferation of the picocyanobacterium, *Synechococcus elongatus,* to reduced flow (Philps et al. 1999, Badylak & Phlips, 2004). While the presumed reduced circulation may certainly play a role in promoting picoplankton growth in the interior canals, it isn't the only factor in effect. Warmer temperatures and longer residence times, attributes associated with residential canals, have been linked with the proliferation of picocyanobacterial blooms in Pensacola Bay (Fl, USA) (Phlips et al., 1999) whereas picoeukaryotes have been associated with higher nutrients and cooler temperatures (Kuosa, 1991, Gaulke et al. 2010, Pulina et al., 2017). While picoplankton were present during all seasons sampled, both groups were positively correlated with temperature in the Padre Island Canals and experienced significantly lower biovolumes in the winter. Picoplankton biovolumes were highest in fall, which is partially aligned with what other studies have observed. A study of Mediterranean lagoons reported picoeukaryotes were highest in the fall, and picocyanobacterial were highest in the summer (Pulina et al., 2017). During the February freeze picoplankton biovolumes were greatly reduced, especially those of picocyanobacteria.

Despite the interconnectivity of the system, the appearance of the cyanobacterium, *Trichodesmium*, at site 1 but not sites 2 and 3 also suggests distinct environmental differences between the mouth and interior canals. *Trichodesmium* is commonly found in the Gulf of Mexico from February to August (King et al., 1950) and has been linked to red tide blooms due to its production of dissolved nitrogen (Sipler et al., 2013). A study investigating *Trichodesmium*

abundances in the Changjiang Estuary (China) found higher concentrations of the cyanobacteria in areas with lower nutrient levels and light availability, but higher salinities and temperatures (Jiang et al., 2017). Additionally, *Trichodesmium* was less abundant in eutrophic sections of the estuary where the salinity was lower (Jiang et al., 2017). Similarly, *Trichodesmium* was only observed at site 1 in this study, which experienced the highest average salinities and lowest nutrient levels throughout the study which may have been more conducive to the cyanobacteria. The rain events that occurred in early May could have led to the demise of *Trichodesmium* in site 1, as it was not observed at any other point during the study.

From February 14th-20th, 2021, Corpus Christi experienced record lows with temperatures ranging from -8.3 to -1.6 ℃. Freeze events do not often occur often along the southern coast of Texas. However, when freeze events do develop temperatures tend to quickly drop in shallow bays leading to fish kills (Buskey et al., 1997). The interior canals experienced their lowest temperatures during February. The freeze conditions that occurred in February 2021 led to fish kills across the Texas coast, with estimates of about 3.8 million fish impacted (TPWD, 2021). Dead fish were observed at all three sites in February following the freeze. However, more dead fish were observed in the interior canals during this time, particularly at Site 3 (Cutajar, pers. obs.). This may have been due to the canals constricted nature, which caused dead fish to concentrate in them. Precipitation rates were lowest during the month of February and all three sites experienced high salinity and no obvious salinity stratification. The interior canals experienced elevated N+N and ammonium during this time. Previous studies showed that remineralization of nutrients from fish kills could trigger phytoplankton growth (Vargo et al., 2008; Walsh et al., 2009). In Texas, previous fish killing freeze events, like the 1989 cold snap in Laguna Madre, were followed by high ammonium levels and a brown tide algal bloom (Buskey

et al. 1997). Ammonium was also found to be a primary compound released during red tide-induced fish kills, but microbial remineralization can make a variety of compounds from decaying fish bioavailable (Killberg-Thoreson et al. 2014). During the freeze recorded in this study, all three sites experienced increased phytoplankton biovolume and two saw increased chlorophyll. However, unlike the 1989 Laguna Madre freeze that coincided with a brown tide algal bloom development, in this case, diatoms dominated the post freeze phytoplankton community.

In May, the study area experienced heavy rainfall due to a tropical disturbance. This was followed by over seven inches of rain in early July 2021 and over eight inches of rain in early October. The rainfall from each of these events caused a reduction in salinity, particularly for the interior canal sites. Site 1 never experienced salinity levels below 20 and did not experience stratification, whereas the decrease in salinity created instances of stratification for sites 2 and 3. The interior canals also experienced increases in orthophosphate with site 2 having the highest recorded orthophosphate during these two periods (Fig. 7). The same pattern was observed for N+N values (Fig. 8). Ammonium also increased for all three sites, especially site 2, but was not as high as it was during the February freeze (Fig. 9). In May and July, phytoplankton biovolume decreased immediately following the heavy rain, suggesting that while the rain washed in additional nutrient sources, it also had the effect of flushing out the preexisting phytoplankton (Fig. 15). While total biovolumes did initially decrease following rainy spring and summer events, the phytoplankton composition began to change, especially in the interior canal sites. In the early spring, picoeukaryotes were the dominant phytoplankton group for the interior canal sites. However, when the rain picked up on May 15th, phytoplankton composition shifted to diatom dominance at site 2. It is possible that the rainfall had a flushing effect on the

picoeukaryotes; however, the effect was less pronounced at site 3 which maintained a dominance of picoeukaryotes and picocyanobacteria over diatoms. Studies of Florida bays reported increases of picocyanobacteria in the summer following rain events that reduced salinities (Putland & Iverson, 2007), and picoeukaryotes have been shown to be stimulated by freshwater pulses (Gaulke et al. 2010). In between the May and July rain events, total biovolume increased, with site 3 experiencing the highest recorded biovolume on June 24th, 2021 (Fig. 30). Thus, there may have been a lag effect in terms of phytoplankton biomass accumulation that resulted from the balance of nutrient inputs and flushing. Interestingly, Euglenoids are associated with influxes on freshwater and eutrophication (Nunes et al., 2018) but may also be susceptible to hydrologic displacement (Roelke et al., 2013). The rain in May could have created favorable nutrient conditions for the bloom, since Euglenoids were positively correlated with ammonium and N+N that all increased that month. Temperature is also known to affect Euglenoid growth rates, with increases reportedly observed in *E. gracilis* growth at temperatures of 25 °C and 30 °C (Ko et al. 2019). The surface temperature at site 3 was 30.5 °C during the Euglenoid spike. The Euglenoid population decreased following increased rainfall in early July. It is possible that the bloom could have been washed out when the rains picked up in July, or the addition of freshwater created unfavorable growth conditions (Tan et al. 2019).

While a harmful algal bloom was not reported during the sampling period it is worth noting that several of the genera identified in the Padre Island Canal system are on the UNESCO List of Harmful Algae. Scanning electron microscopy was used to further identify potentially harmful species which included three complexes of the diatom *Pseudonitzschia* (*delicatissima*, *seriata*, and *pungens*), and dinoflagellates *Prorocentrum micans* and *Pyrodrinium bahamense* (Figs. 32-34). Other potentially harmful dinoflagellates identified included *Polykrikos*,

Dinophysis, *Heterocapsa*, *Karlodinium*, *Gonyaulax*. Additionally, the raphidophytes *Fibrocapsa japonica* and *Chattonella* were observed in live samples. Furthermore, the Texas Park and Wildlife Department lists the dinoflagellate, *Akashiwo sanguinea,* which was also observed at all sites, as a potential HAB former. Although these genera did not form bloom level concentrations, it is still important to understand what conditions could promote bloom development in the future.

Conclusions – Recommendations for future research and managers

The 2021 sampling period was characterized by several extreme events, including the February freeze, Tropical Storm Elsa in July and the category 1 Hurricane Nicholas in mid-September. In order to properly assess the short- and long-term effects of these events on phytoplankton communities it is important to have hydrographic, nutrient, and phytoplankton monitoring efforts already in place. The environmental conditions of a waterbody before a storm impacts what phytoplankton can bloom in the aftermath of such events (Wetz & Paerl, 2008). Previous studies have documented how even changes in weather (periods of reduced rainfall vs. periods of increased precipitation) can drastically alter phytoplankton communities (Badylak & Phlips, 2004). Since phytoplankton are highly dynamic, fast-growing organisms, there is a demand for higher frequency of sampling. Some studies recommend daily sampling to capture the true variation in phytoplankton (Dubelaar et al., 2004), other studies have investigated machine learning instruments (Derot et al, 2020), and research ships of opportunity (Rantajärvi et al., 1998) to find more feasible ways to adequately capture spatial and temporal trends of phytoplankton blooms. However, since there is no universal standard for sampling frequency, we recommend monthly sampling, with increases when possible, especially in the spring and summer for semi-arid waterbodies.

Continuous long-term monitoring of estuaries and sub-basins such as canals will better inform communities and coastal managers. If the design of canals is influencing nutrients and phytoplankton composition, which this study suggests, then perhaps changes in future design plans can help ameliorate some of the unwanted side effects. Previous studies that evaluated dead-end canals in Maryland and Delaware recommended that newly constructed canal systems take different shapes into consideration, like more rounded corners, and additional connections for enhanced flushing rates (Maxted et al., 1997). Other studies have also admonished the dead end canal structure in favor for systems with increased interconnectivity to other canals and locations that are parallel to wind patterns for improved flow and water quality (Lindall & Trent, 1975; Marvin et al., 1990). Although flow and flushing rate were not examined in this study, they may contribute to differences in the physical and chemical nature of the canals as well as the phytoplankton composition and therefore need to be examined. Previous studies have demonstrated the importance of flow in determining which phytoplankton have a competitive advantage (Hall et al., 2013). For instance, systems that are regularly flushed tend to favor fast growing phytoplankton, like diatoms. Similarly, systems with reduced flushing rates have been linked to HABs (Paerl, 1988, Anderson et al., 2002, Lewitus et al., 2003).

For canals already in existence, mitigation strategies like fountains, could help oxygenate the system and reduce the stratification observed during rainfall events (Koweek et al., 2020; Maxted et al., 1997). Low oxygen conditions can alter sediment biogeochemistry and have been linked to nutrient loading, particularly phosphate, from the bottom sediments (Pearl et al. 1998, Foster & Fulweiler, 2019). Hypoxia induced phosphate loading can alter nutrient regimes and promote primary productivity, thus increasing the phytoplankton growing season and organic matter buildup (Foster & Fulweiler, 2019). It is worth noting that while this study was being

conducted, the Padre Island canals were undergoing the construction of a new bridge and canal that will connect Packery Channel to Padre Island. In addition to connectivity, the hope is that the new canal will improve circulation and water quality via connection to the Gulf of Mexico reducing the need for aerators in the canal system (Rankin, 2020). Improved flow could help mitigate nutrient runoff associated with urban canal systems.

Fertilizer runoff has been associated with eutrophication of urban waterbodies and may also be a source of external nutrient loading to the Padre Island Canal System. Previous studies of nitrogen loading to estuarine systems using stable isotopes were able to detect even low levels of land based nitrogen to the food web (Carmichael et al., 2004.). In another study, isotope ratios collected from marsh grasses determined that increases in population density were correlated with anthropogenic nitrogen sources (Bannon & Roman, 2008). Similarly, isotopic testing could reveal the source of nutrients in the Padre Island canal system, to determine if the interior canals proximity to urbanized areas may be affecting the type of nutrients that enter these systems during rainfall events. Moreover, isotope testing could shed light on nutrient cycling, and how it may differ based on location, in the canals. Knowledge of nutrient sources will also help understand why certain phytoplankton groups develop. Once nutrient sources are determined, best management practices, like a fertilizer ordinance, could be applied to residential canal areas in South Texas. Urban nutrients have contributed to the eutrophication of South Florida estuaries, which led to a fertilizer ordinance that helped reduced total nitrogen and phosphorus levels in the two years following enactment of the ordinance (Motsch, 2018). Other best management practices, like planting vegetative buffers, have been effective in reducing nitrogen inputs to river-fed agricultural canals (Castaldelli et al., 2015), but a similar logic could be applied to estuarine-fed residential canals.

Ultimately, canals are important urban bodies that are expanding worldwide but are understudied ecosystems. This project demonstrated that two interior canal sites experienced unique nutrient and phytoplankton composition when compared to the mouth of the canal system. Manmade alterations to estuarine environments create unique habitats at the intersection of environmental and human health. Therefore, continued research and monitoring is important to understand these systems especially in the face of climate change.

REFERENCES

Anderson, D. M., Gilbert, P. M., & Burkholder, J. M. 2002. Harmful algal blooms and eutrophication: Nutrient sources, composition, and consequences. *Estuarine Research Federation Estuaries* 25 (4b): 704-726. doi:10.1007/BF02804901

Badylak, S., & Phlips, E. J. 2004. Spatial and temporal patterns of phytoplankton composition in a subtropical coastal lagoon, the Indian River Lagoon, Florida, USA. *Journal of Plankton Research* 26 (10): 1229–1247. doi:10.1093/PLANKT/FBH114

Bannon, R. O., & Roman, C. T. 2008. Using stable isotopes to monitor anthropogenic nitrogen inputs to estuaries. *Ecological Applications* 18(1): 22-20. doi:10.1890/06-2006.1

Baustian, M. M., Jeanette, G., Hansen, A., & Robinson, K. 2014. Linking the bottom to the top in aquatic ecosystems: mechanisms and stressors of benthic-pelagic coupling. In *Eco-DAS X*, ed. P. F. Kemp, 38–60. Association for the Sciences of Limnology and Oceanography. doi:10.4319/ecodas.2014.978-0-9845591-4-5.38

Bec, B., Husseini-Ratrema, J., Collos, Y., Souchu, P., & Vaquer, A. 2005. Phytoplankton seasonal dynamics in a Mediterranean coastal lagoon: Emphasis on the picoeukaryote community. *Journal of Plankton Research* 27(9): 881–894. doi:10.1093/plankt/fbi061

Behrenfeld, M. J., & Boss, E. 2006. Beam attenuation and chlorophyll concentration as alternative optical indices of plankton biomass. *Journal of Marine Research* 64(3): 431-451. doi:10.1357/002224006778189563

Bonilla, S., Conde, D., Aubriot, L., & Pérez, M. D. C. 2005. Influence of hydrology on phytoplankton species composition and life strategies in a subtropical coastal lagoon periodically connected with the Atlantic Ocean. *Estuaries* 28(6): 884–895. doi:10.1007/BF02696017

Bricker, S. B., Longstaff, B., Dennison, W., Jones, A., Boicourt, K., Wicks, C., & Woerner, J. 2008. Effects of nutrient enrichment in the nation's estuaries: A decade of change. *Harmful Algae* 8: 21–32. doi:10.1016/j.hal.2008.08.028

Boynton, W. R., Ceballos, M. A. C., Bailey, E. M., Hodgkins, C. L. S., Humphrey, J. L., & Testa, J. M. 2018. Oxygen and nutrient exchanges at the sediment-water interface: A global synthesis and critique of estuarine and coastal data. *Estuaries and Coasts* 41(2): 301–333. doi:10.1007/s12237-017-0275-5.

Buskey, E. J., Montagna, P. A., Amos, A. F., & Whitledge, T. E. 1997. Disruption of grazer populations as a contributing factor to the initiation of the Texas brown tide algal bloom. *Limnology and Oceanography* 42(5.2): 1215–1222. doi:10.4319/lo.1997.42.5_part_2.1215

Carmichael, R. H., Annett, B., & Valiela, I. 2004. Nitrogen loading to Pleasant Bay, Cape Cod: Application of models and stable isotopes to detect incipient nutrient enrichment of estuaries. *Marine Pollution Bulletin* 48: 137–143. doi:10.1016/S0025-326X(03)00372-2

Castaldelli, G., Soana, E., Racchetti, E., Vincenzi, F., Fano, E. A., & Bartoli, M. 2015. Vegetated canals mitigate nitrogen surplus in agricultural watersheds. *Agriculture, Ecosystems and Environment* 212: 253–262. doi:10.1016/j.agee.2015.07.009

Chan, A. T. 1980. Comparative physiological study of marine diatoms and dinoflagellates in relation to irradiance and cell size. II. Relationship between photosynthesis, growth, and carbon/chlorophyll a ratio. *Journal of Phycology* 16(3): 428–432. doi:10.1111/j.1529-8817.1980.tb03056.x

Cloern, J. E. 2001. Our evolving conceptual model of the costal eutrophication problem. *Marine Ecology Progress Series* 210: 223-253. doi:10.3354/meps210223

Cloern, J. E. 2018. Why large cells dominate estuarine phytoplankton. *Limnology and*

Oceanography 63: S392–S409. doi:10.1002/lno.10749

Corliss, J., & Trent, L. 1971. Comparison of phytoplankton production between natural and altered areas in West Bay, Texas. *Fishery Bulletin* 69(4): 829–833.

Dellapenna, T. M., Fielder, B., Noll, C. J., & Savarese, M. 2015. Geological responses to urbanization of the Naples Bay estuarine system, Southwestern Florida, USA. *Estuaries and Coasts* 28:S81–S96. doi:10.1007/s12237-013-9704-2

Derot, J., Yajima, H., Schmitt, F. G. 2020. Benefits of machine learning and sampling frequency on phytoplankton bloom forecasts in coastal area. Ecological Informatics 60: 1-44. doi:10.1016/j.ecoinf.2020.101174

Dillon, P. J. 1975. The phosphorus budget of Cameron Lake, Ontario: The importance of flushing rate to the degree of eutrophy of lakes. *Limnology and Oceanography* 20(1): 28–39. doi:10.4319/lo.1975.20.1.0028

Dubelaar, G. B. J., Geerders, P. J. F., and Jonker, R. R. 2004. High frequency monitoring reveals phytoplankton dynamics. *Journal of Environmental Monitoring* 6: 946-952. doi: 10.1039/B409350J

Falkowski, P. G. 1980. Light-shade adaptation in marine phytoplankton. In *Primary Productivity in the Sea,* ed. Falkowski, P. G. 99–119. Plenum Press, New York. doi:10.1007/978-1-4684-3890-1_6

Flint, R. W. 1984. Phytoplankton production in the Corpus Christi Bay estuary. *Contributions in Marine Science* 27: 65–83.

Foster, S. Q., & Fulweiler, R. W. 2019. Estuarine sediments exhibit dynamic and variable biogeochemical responses to hypoxia. *Journal of Geophysical Research: Biogeosciences* 124(4):737-758. doi:10.1029/2018JG004663.

Gaulke, A. K., Wetz, M. S., Paerl, H. W. 2010. Picophytoplankton: A major contributor to planktonic biomass and primary production in a eutrophic, river-dominated estuary. *Estuarine, Coastal and Shelf Science*, 90(1): 45-54. doi:10.1016/j.ecss.2010.08.006

Glibert, P. M., & Burkholder, J. M. 2006. The complex relationships between increases in fertilization of the Earth, coastal eutrophication and proliferation of harmful algal blooms. *Ecology of Harmful Algae* 341–354. doi:10.1007/978-3-540-32210-8_26

Goodwin, C. R. 1991. Simulation of the effects of proposed tide gates on circulation, flushing, and water quality in residential canals, Cape Coral, Florida. U.S. Geological Survey 91-237. doi:10.3133/ofr91237

Hall, N. S., Paerl, H. W., Peierls, B. L., Whipple, A. C., & Rossignol, K. L. 2013. Effects of climatic variability on phytoplankton community structure and bloom development in the eutrophic, microtidal, New River Estuary, North Carolina, USA. *Estuarine, Coastal and Shelf Science* 117: 70–82. doi:10.1016/J.ECSS.2012.10.004

Hillebrand, H., C.-D. Durselen, D. Kirschtel, U. Pollingher, and T. Zohary. 1999. Biovolume calculation for pelagic and benthic macroalgae. *Journal of Phycology* 35: 403–424. doi:10.1046/j.1529-8817.1999.3520403.x

Ivey, J. E., Wolny, J. L., Heil, C. A., Murasko, S. M., Brame, J. A., & Parks, A. A. 2020. Urea inputs drive picoplankton blooms in Sarasota Bay, Florida, U.S.A. *Water* 12(10), 2755. doi:10.3390/w12102755

Jiang, Z., Chen, J., Zhou, F., Zhai, H., Zhang, D., & Yan, X. 2017. Summer distribution patterns of *Trichodesmium* spp. in the Changjiang (Yangtze River) Estuary and adjacent East China Sea shelf. *Oceanologia* 59(3): 248–261. doi:10.1016/J.OCEANO.2017.02.001

Kelly, L. A., & Hassall, C. 2018. Inland waters the spatial ecology of phytoplankton blooms in

UK canals. *Inland Waters* 8(4): 422–433. doi:10.1080/20442041.2018.1482152

Kemp, W. M., Sampou, P., Caffrey, J., Mayer, M. 1990. Ammonium recycling versus denitrification in Chesapeake Bay sediments. *Limnology and Oceanography* 35(7): 1545-1563. doi:10.4319/lo.1990.35.7.1545

Killberg-Thoreson, L., Sipler, R. E., Heil, C. A., Garrett, M. J., Roberts, Q. N., & Bronk, D. A. 2014. Nutrients released from decaying fish support microbial growth in the eastern Gulf of Mexico. *Harmful Algae* 38(C): 40–49. doi:10.1016/j.hal.2014.04.006

King, J. E. 1950. A preliminary report on the plankton of the west coast of Florida. *Quarterly Journal of the Florida Academy of Sciences* 12:109–137.

Ko, S., Speckmaier, S., & Wang, N. 2019. The effect of temperature on the growth rate of Euglena gracilis. The Expedition, 9, 1–19.

Koweek, D. A., García-Sánchez, C., Brodrick, P. G., Gassett, P., & Caldeira, K. 2020. Evaluating hypoxia alleviation through induced downwelling. *Science of the Total Environment* 719:1-12. doi:10.1016/J.SCITOTENV.2020.137334

Kuosa, H. 1991. Picoplanktonic algae in the northern Baltic Sea: seasonal dynamics and flagellate grazing. *Marine Ecology Progress Series* 73(2–3): 269–276. doi:10.3354/MEPS073269

Lehman, P. W. 1981. Comparison of chlorophyll a and carotenoid pigments as predictors of phytoplankton biomass. *Marine Biology* 65:237-244. doi:10.1007/BF00397117

Lewitus, A. J., Baruch, B. W., Schmidt, L. B., Mason, L. J., Kempton, J. W., Wilde, S. B., Wolny, J. L., Williams, B. J., Hayes, K. C., Hymel, S. N., Keppler, C. J., & Ringwood, A. H. 2003. Harmful algal Blooms in South Carolina residential and golf course ponds. *Population and Environment* 24(5): 387-413.

Lewitus, A. J., White, D. L., Tymowski, R. G., Geesey, M. E., Hymel, S. N., & Noble, P. A. 2005. Adapting the CHEMTAX method for assessing phytoplankton taxonomic composition in southeastern U.S. estuaries. *Estuaries* 28(1): 160–172. doi:10.1007/BF02732761

Lewitus, A. J., Brock, L. M., Burke, M. K., DeMattio, K. A., & Wilde, S. B. 2008. Lagoonal stormwater detention ponds as promoters of harmful algal blooms and eutrophication along the South Carolina coast. *Harmful Algae* 8(1): 60–65. doi:10.1016/j.hal.2008.08.012

Lindall, W. N. J., & Trent, L. 1975. Housing development canals in the coastal zone of the Gulf of Mexico: Ecological consequences, regulations, and recommendations. *Marine Fisheries Review* 1163:19-24.

Lomas, M. W., & Gilbert, P. M. 2000. Comparisons of nitrate uptake, storage, and reduction in marine diatoms and flagellates. *Journal of Phycology* 36(5): 903–913. doi:10.1046/j.1529-8817.2000.99029.x

Marvin, K. T., Baxter, K. N., & Scott, E. 1990. Effects of aligning waterfront housing development canals with prevailing summer winds and installing a circulation canal and culverts. NOAA Technical Memorandum. NMFS – SEFC – 268: 2-28.

Maxted, J. R., Weisberg, S. B., Chaillou, J. C., Eskin, R. A., & Kutz, F. W. 1997. The ecological condition of dead-end canals of the Delaware and Maryland coastal bays. *Estuaries* 20(2): 319–327. doi:10.2307/1352347

Mitbavkar, S., Rajaneesh, K. M., Anil, A. C., & Sundar, D. 2012. Picophytoplankton community in a tropical estuary: Detection of *Prochlorococcus*-like populations. *Estuarine, Coastal and Shelf Science* 107: 159–164. doi:10.1016/j.ecss.2012.05.002

Motsch, K. 2018. Improving estuarine water quality in South Florida: A quantitative evaluation

of the efficacy of a local nutrient ordinance. Doctoral dissertation, Columbus, GA: Columbus State University.

Murrell, M. C., & Lores, E. M. 2004. Phytoplankton and zooplankton seasonal dynamics in a subtropical estuary: Importance of cyanobacteria. *Journal of Plankton Research* 26(3): 371–382. doi:10.1093/PLANKT/FBH038

Neumann, B., Vafeidis, A. T., Zimmermann, J., & Nicholls, R. J. 2015. Future coastal population growth and exposure to sea-level rise and coastal flooding - A global assessment. *PLoS ONE* 10(3):1-34. doi:10.1371/journal.pone.0118571

Ning, X., Cloern, J. E., & Cole, B. E. 2000. Spatial and temporal variability of picocyanobacteria *Synechococcus* sp. in San Francisco Bay. *Limnology and Oceanography* 45(3): 695–702. doi:10.4319/lo.2000.45.3.0695

Nixon, S. W. 1988. Physical energy inputs and the comparative ecology of lake and marine ecosystems. *Limnology and Oceanography* 33(4.2): 1005-1025. doi:10.4319/lo.1988.33.4part2.1005

Nunes, M., Adams, J. B., & Rishworth, G. M. 2018. Shifts in phytoplankton community structure in response to hydrological changes in the shallow St Lucia Estuary. *Marine Pollution Bulletin* 128: 275–286. doi:10.1016/j.marpolbul.2018.01.035

Paerl, H. W. 1988. Nuisance phytoplankton blooms in coastal, estuarine, and inland waters. *Limnology and Oceanography* 33(4.2):823-847.

Paerl, H. W., Pickney, J. L., Fear, J. M., Peierls, B. L. 1998. Ecosystem responses to internal and watershed organic matter loading: consequences for hypoxia in the eutrophying Neuse River Estuary, North Carolina, USA. *Marine Ecology Progress Series* 166: 17-25.

Paerl, H. W., Valdes, L. M., Joyner, A. R., Peierls, B. L., Piehler, M. F., Riggs, S. R., Christian,

R. R., Eby, L. A., Crowder, L. B., Ramus, J. S., Clesceri, E. J., Buzzelli, C. P., & Luettich, R. A. 2006. Ecological response to hurricane events in the Pamlico Sound system, North Carolina, and implications for assessment and management in a regime of increased frequency. *Estuaries and Coasts* 29(6):1033–1045. doi:10.1007/bf02798666

Paerl, H. W. 2010. Phytoplankton community indicators of short- and long- term ecological change in the anthropogenically and climatically impacted Neuse River Estuary, North Carolina, USA. *Estuaries and Coasts* 33(2010): 485-497.

Paerl, H. W. and Scott, J. T. 2010. Throwing fuel on the fire: Synergistic effects of excessive nitrogen inputs and global warming on harmful algal blooms. *Environmental Science and Technology* 44(20): 7756–7758. doi:10.1021/es102665e

Phlips, E. J., Badylak, S. and Lynch, T. C. 1999. Cyanobacterial blooms in Florida Bay. *Limnology and Oceanography* 44: 1166–1175.

Pulina, S., Satta, C. T., Bachisio, &, Padedda, M., Bazzoni, A. M., Sechi, N., & Lugliè, A. 2017. Picophytoplankton seasonal dynamics and interactions with environmental variables in three Mediterranean coastal lagoons. *Estuaries and Coasts* 40: 469–478. doi:10.1007/s12237-016-0154-5

Putland, J. N., & Iverson, R. L. 2007. Phytoplankton biomass in a subtropical estuary: Distribution, size composition, and carbon: Chlorophyll ratios. *Estuaries and Coasts* 30(5): 878–885. doi:10.1007/BF02841341

Rankin, Dale. 2020. Island Report: Work begins on Padre Island Canal. *3News*, May 20.

Roelke, D. L., Li, H. P., Hayden, N. J., Miller, C. J., Davis, S. E., Quigg, A., & Buyukates, Y. 2013. Co-occurring and opposing freshwater inflow effects on phytoplankton biomass, productivity and community composition of Galveston Bay, USA. *Marine Ecology*

Progress Series 477: 61–76. doi:10.3354/MEPS10182

Sipler, R., Bronk, D., Seitzinger, S., Lauck, R., McGuinness, L., Kirkpatrick, G., Heil, C., Kerkhof, L., & Schofield, O. 2013. *Trichodesmium*-derived dissolved organic matter is a source of nitrogen capable of supporting the growth of toxic red tide *Karenia brevis*. *Marine Ecology Progress Series* 483, 31–45. doi:10.3354/meps10258

Smayda, T. J. 1997. Harmful algal blooms: Their ecophysiology and general relevance to phytoplankton blooms in the sea. *Limnology and Oceanography* 45((5 II)): 1137–1153.

Sun, J., and D. Liu. 2003. Geometric models for calculating cell biovolume and surface area for phytoplankton. *Journal of Plankton Research* 25: 1331-1346. doi:10.1093/plankt/fbg096

Tan, Y., Li, J., Zhang, L., Chen, M., Zhang, Y., & An, R. 2019. Mechanism underlying flow velocity and its corresponding influence on the growth of *Euglena gracilis,* a dominant bloom species in reservoirs. *Environmental Research and Public Health*, 16(23): 1–15. doi:10.3390/ijerph16234641

Texas Parks and Wildlife Division. 2021. Winter Storm Coastal Fisheries Impacts.

Utermöhl, H. 1931. Neue Wege der quantitativen Erfassung des Planktons (mit besonderer des Berücksichtigung Ultraplanktons). *Verhandlungen der Internationalen Vereinigung für Theoretische und Angewandte Limnologie* 5: 567-596.

Utermöhl, H. 1958. Zur Vervollkommnung der quantitativen Phytoplankton-Methodik. *Verhandlungen der Internationalen Vereinigung für Theoretische und Angewandte Limnologie* 9: 1-38.

Vargo, G. A., Heil, C. A., Fanning, K. A., Dixon, L. K., Neely, M. B., Lester, K., Ault, D., Murasko, S., Havens, J., Walsh, J., & Bell, S. 2008. Nutrient availability in support of *Karenia brevis* blooms on the central West Florida Shelf: What keeps *Karenia* blooming?

Continental Shelf Research 28: 73–98. doi:10.1016/j.csr.2007.04.008

Verity, P. G. 2010. Expansion of potentially harmful algal taxa in a Georgia Estuary (USA). *Harmful Algae* 9(2): 144–152. doi:10.1016/j.hal.2009.08.009

Wachnicka, A., Browder, J., Jackson, T., Louda, W., Kelble, C., Abdelrahman, O., Stabenau, E., & Avila, C. 2020. Hurricane Irma's impact on water quality and phytoplankton communities in Biscayne Bay (Florida, USA). *Estuaries and Coasts* 43(5): 1217–1234. doi:10.1007/s12237-019-00592-4

Walsby, A. E., Hayes, P. K., & Boje, R. 1995. The gas vesicles, buoyancy and vertical distribution of cyanobacteria in the Baltic Sea. *European Journal of Phycology* 30(2): 87–94. doi:10.1080/09670269500650851

Walsh, J. J., Weisberg, R. H., Lenes, J. M., Chen, F. R., Dieterle, D. A., Zheng, L., Carder, K. L., Vargo, G. A., Havens, J. A., Peebles, E., Hollander, D. J., He, R., Heil, C. A., Mahmoudi, B., & Landsberg, J. H. 2009. Isotopic evidence for dead fish maintenance of Florida red tides, with implications for coastal fisheries over both source regions of the West Florida shelf and within downstream waters of the South Atlantic Bight. *Progress in Oceanography* 80(1–2): 51–73. doi:10.1016/j.pocean.2008.12.005

Waltham, N. J., & Connolly, R. M. 2011. Global extent and distribution of artificial, residential waterways in estuaries. *Estuarine, Coastal and Shelf Science* 94(2): 192–197. doi:10.1016/j.ecss.2011.06.003

Wetz, M. S., & Paerl, H. W. 2008. Estuarine phytoplankton responses to hurricanes and tropical storms with different characteristics (trajectory, rainfall, winds). *Estuaries and Coasts* 31(2): 419–429. doi:10.1007/S12237-008-9034-Y/FIGURES/9

Wilson, G. S. F. R. T. 2010. Coastline Population Trends in the United States 1960 to 2008.

Population Estimates and Projections. P25-1139: 1-27.

Xing, Z., Chua, L. H. C., Miao, H., Imberger, J., & Yang, P. 2018. Wind shielding impacts on water quality in an urban reservoir. *Water Resourse Management* 32: 3549–3561. doi:10.1007/s11269-018-1980-y

Yamada, K., Kazama, Y., Mitra, S., Marukawa, Y., Arashida, R., Abe, T., Ishikawa, T., & Suzuki, K. 2016. Production of a thermal stress resistant mutant Euglena gracilis strain using Fe-ion beam irradiation. Bioscience, Biotechnology, and Biochemistry, 80:8, 1650–1656. doi:10.1080/09168451.2016.1171702

APPENDIX A

SUMMARY OF GENERA AND THEIR ASSOCIATED SHAPE USED FOR BIOVOLUME CALCULATIONS

Genus	Shape	Source
Akashiwo sanguinea	Ellipsoid	Hillebrand et al. (1999) Sun and Liu (2003)
Amphora cf	Elliptic prism constricted	Decided based on observed shape.
Asterionellopsis glacialis	Cylinder cone	Decided based on observed shape.
Bacillaria	Rectangular box	Hillebrand et al. (1999) Sun and Liu (2003)
Bacteriastrum	Cylinder girdle	Sun and Liu (2003)
Chaetoceros	Elliptic prism girdle	Sun and Liu (2003)
Chattonella	Cone halfsphere	Sun and Liu (2003)
Chroomonas	Cone halfsphere	Sun and Liu (2003)
Cochlodinium	Prolate spheroid	Hillebrand et al. (1999)
Coscinodiscus	Cylinder	Hillebrand et al. (1999) Sun and Liu (2003)
Cylindrotheca	Prolate spheroid + 2 cylinders	Hillebrand et al. (1999)
Dinophysis	Ellipsoid	Hillebrand et al. (1999) Sun and Liu (2003)
Ditylum	Prism Triangle	Sun and Liu (2003)
Entomoneis	Elliptic prism constricted	Decided based on observed shape.

Eucampia	Elliptic prism girdle view	Decided based on observed shape.
Euglena	Cone halfsphere cylinder	Sun and Liu (2003)
Fibrocapsa	Prolate spheroid	Hillebrand et al. (1999)
Fragilaria	Elliptic prism girdle	Hillebrand et al. (1999) Sun and Liu (2003)
Gonyaulax	Double cone	Hillebrand et al. (1999)
Guinardia	Cylinder girdle	Sun and Liu (2003)
Gymnodinium	Ellipsoid	Hillebrand et al. (1999) Sun and Liu (2003)
Gyrodinium	Ellipsoid	Hillebrand et al. (1999) Sun and Liu (2003)
Hermesium	Double cone	Decided based on observed shape.
Heterocapsa	Double cone	Hillebrand et al. (1999)
Karenia cf	Ellipsoid	Hillebrand et al. (1999) Sun and Liu (2003)
Katodinium	Cylinder cone	Hillebrand et al. (1999)
Leptocylindrus	Cylinder girdle	Sun and Liu (2003)
Levanderina	Ellipsoid	Sun and Liu (2003)
Licmophora	Gomphonemoid	Hillebrand et al. (1999)
Naviculoid	Elliptic prism	Hillebrand et al. (1999) Sun and Liu (2003)
Nitzschiod	Rectangular box	Decided based on observed shape.
Odontella	Elliptic prism	Hillebrand et al. (1999)
Oxyphysis Oxytoxoides	Double cone	Hillebrand et al. (1999)

Oxyrrhis	Prolate spheroid	Hillebrand et al. (1999)
Paralia	Cylinder	Hillebrand et al. (1999)
Pediastrum	Elliptic prism	Hillebrand et al. (1999)
Phaeodactylum cf	Half-elliptic prism	Hillebrand et al. (1999)
Pleurosigma	Elliptic prism	Decided based on observed shape.
Polykrikos	Ellipsoid	Hillebrand et al. (1999) Sun and Liu (2003)
Prorocentrum micans	Ellipsoid	Hillebrand et al. (1999) Sun and Liu (2003)
Prorocentrum_minium	Ellipsoid	Hillebrand et al. (1999) Sun and Liu (2003)
Protoperidinium	Double cone	Hillebrand et al. (1999) Sun and Liu (2003)
Pseudonitzschia	Rectangular box	Decided based on observed shape.
Pyrodinium	Ellipsoid	Hillebrand et al. (1999)
Rhizosolenia	Cylinder girdle	Decided based on observed shape.
Scenedesmus	Prolate spheroid	Hillebrand et al. (1999)
Scrippsiella	Cone halfsphere	Sun and Liu (2003)
Skeletonema cf	Cylinder 2 halfspheres	Sun and Liu (2003)
Striatella unipunctata	Rectangular box	Decided based on observed shape.
Thalassionema	Rectangular box	Sun and Liu (2003)
Thalassiosira	Cylinder	Hillebrand et al. (1999) Sun and Liu (2003)

Trichodesmium	Cylinder	Hillebrand et al. (1999)
Tripos furca (Ceratium furca)	Ellipsoid 2 cones cylinder	Hillebrand et al. (1999) Sun and Liu (2003)

APPENDIX B

DINOFLAGELLATES OBSERVED IN AUGUST 2021 BY SITE

Dinoflagellate	**Site**
Akashiwo sanguinea	1
Cochlodinium	1, 3
Gyrodinium	1, 2, 3
Katodinium	3
Oxyphysis oxtoxoides	1, 2, 3
Protoperidinium	2, 3
Scrippsiella	1, 2, 3

FIGURES

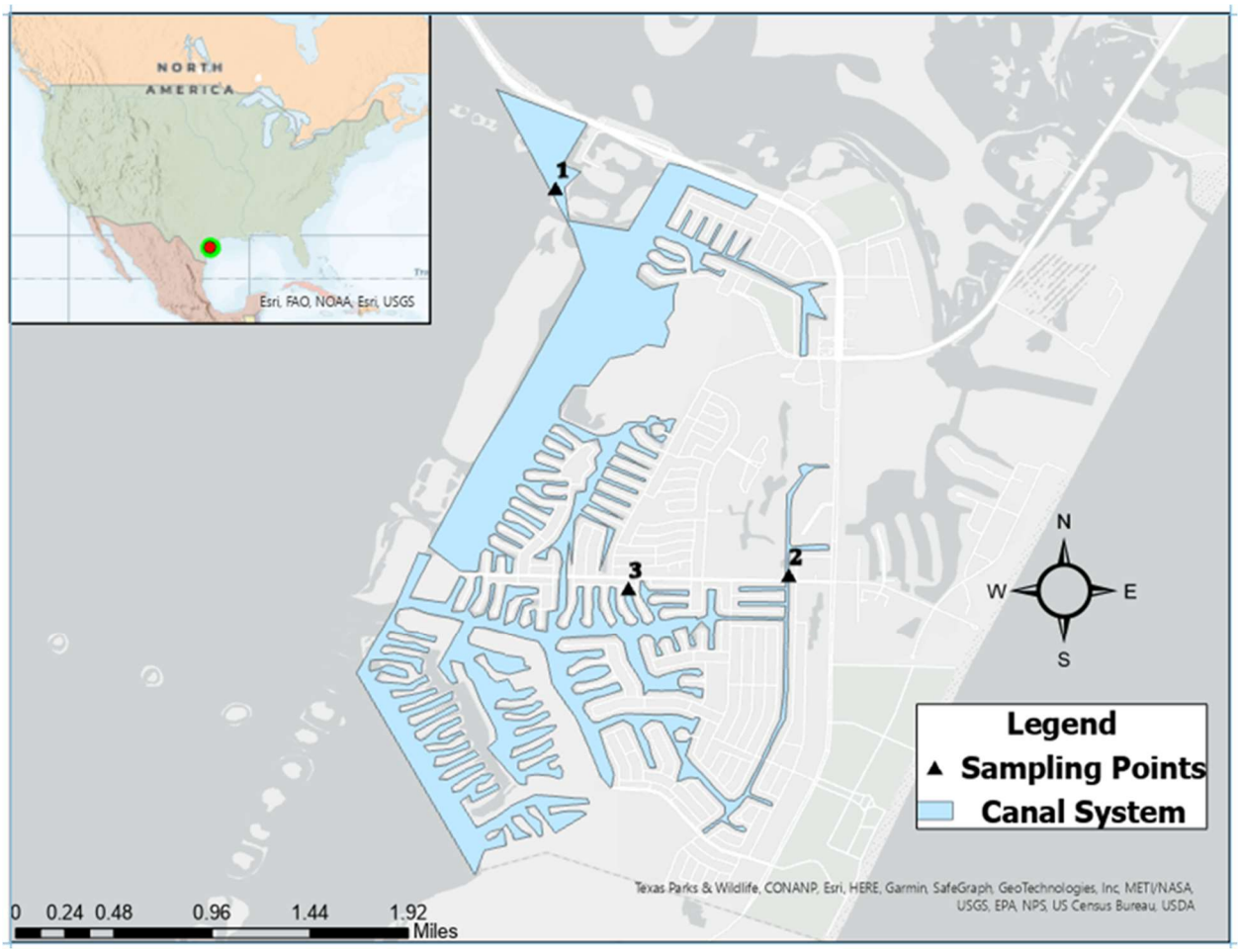

Figure 1: Map of Padre Island Canals

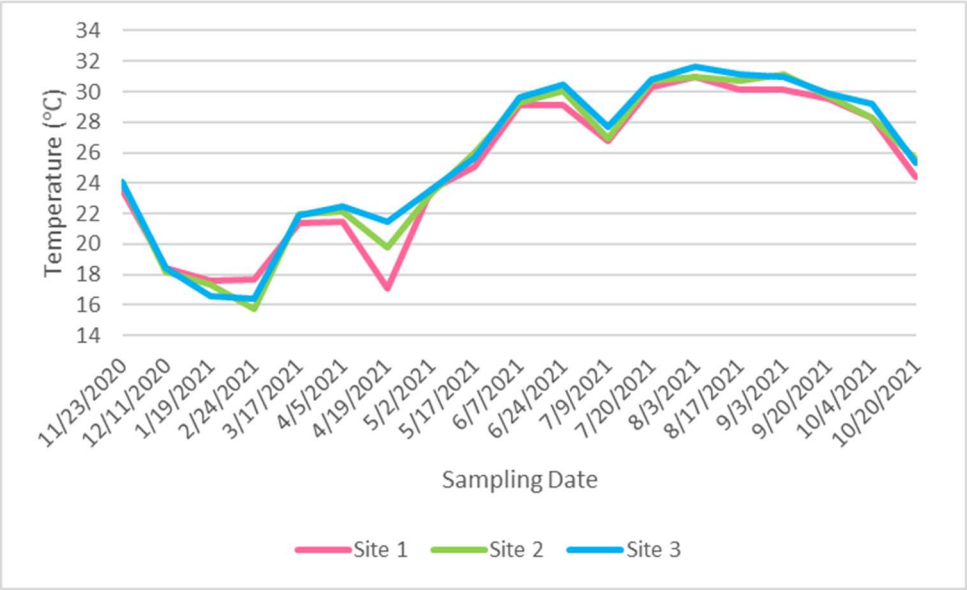

Figure 2: Temperature over time

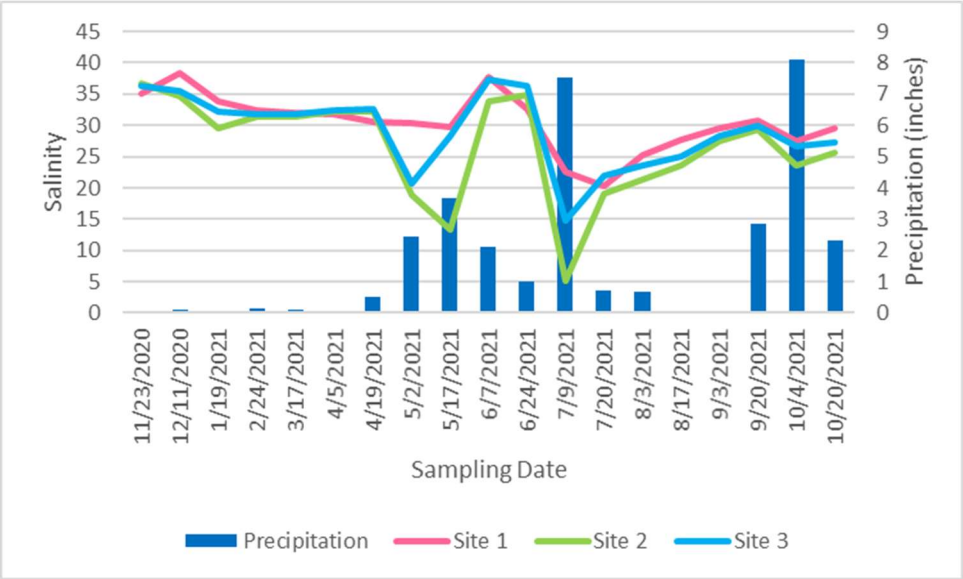

Figure 3: Salinity and precipitation (7-day total) over time

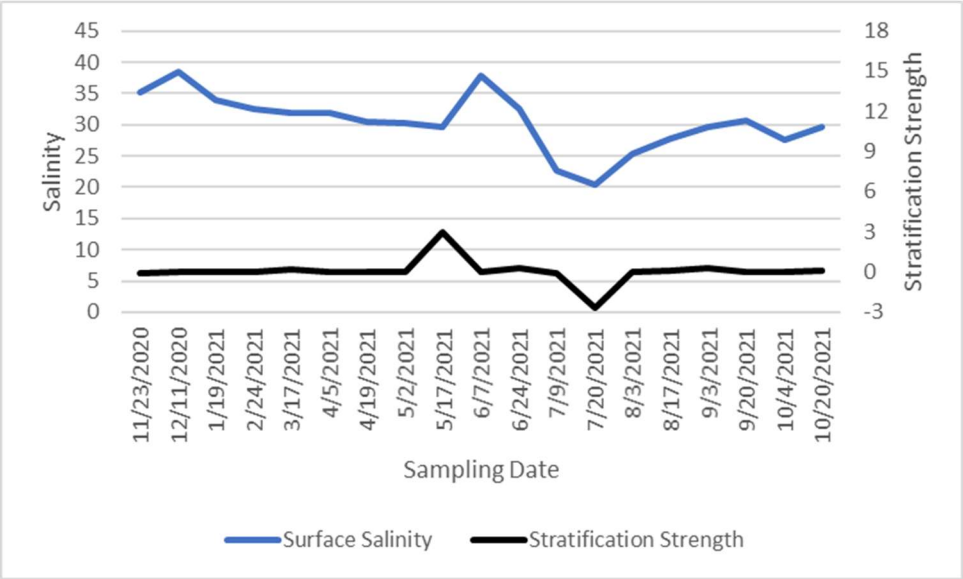

Figure 4: Site 1 stratification strength based on salinity

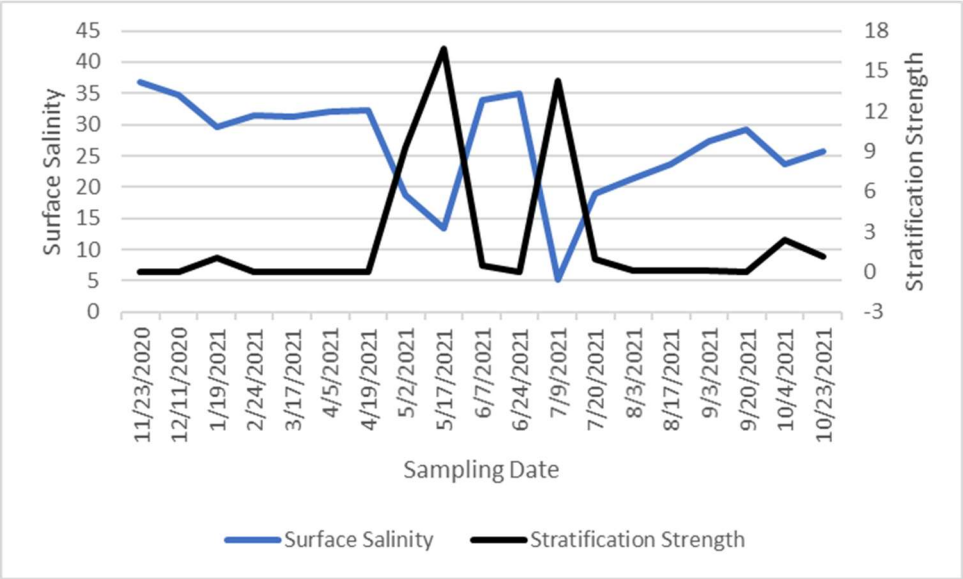

Figure 5: Site 2 stratification strength based on salinity

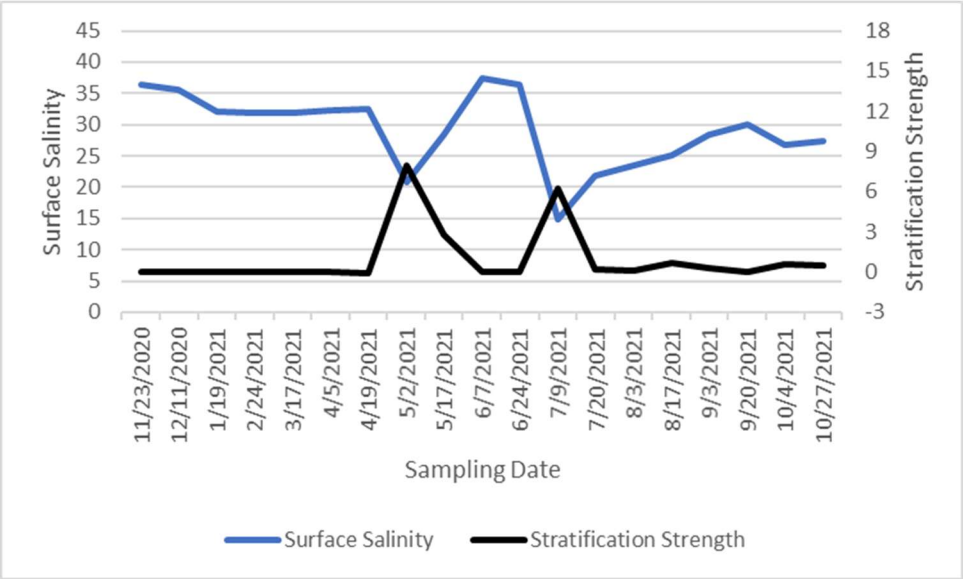

Figure 6: Site 3 stratification strength based on salinity

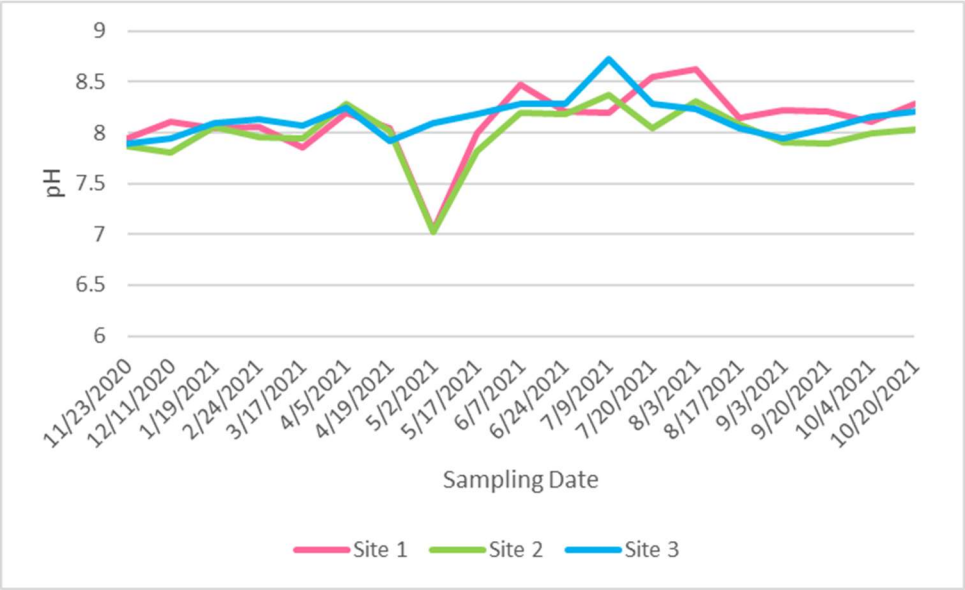

Figure 7: pH over time

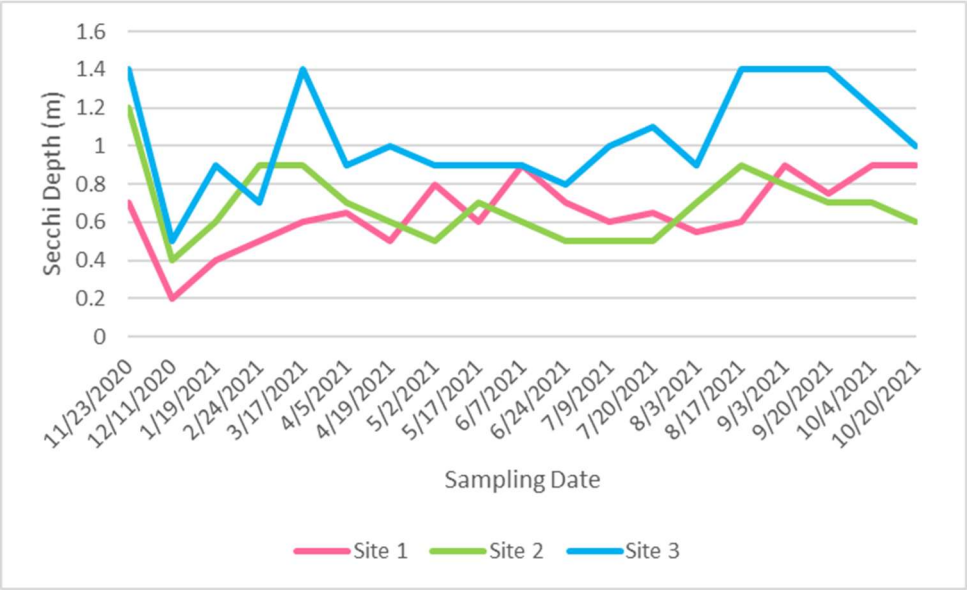

Figure 8: Secchi depths over time

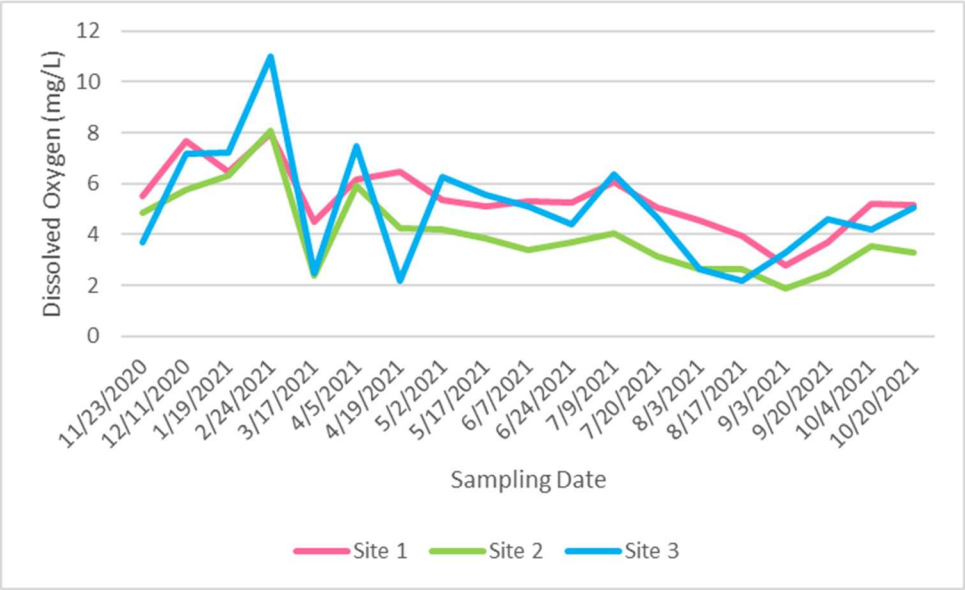

Figure 9: Dissolved oxygen over time

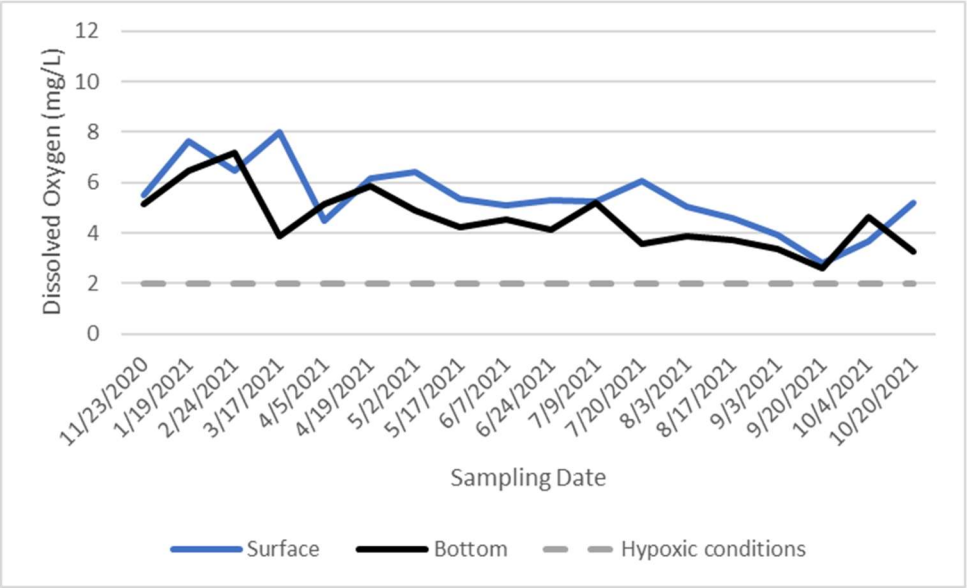

Figure 10: Site 1 surface and bottom dissolved oxygen. Hypoxic conditions when dissolved oxygen < 2mg/L.

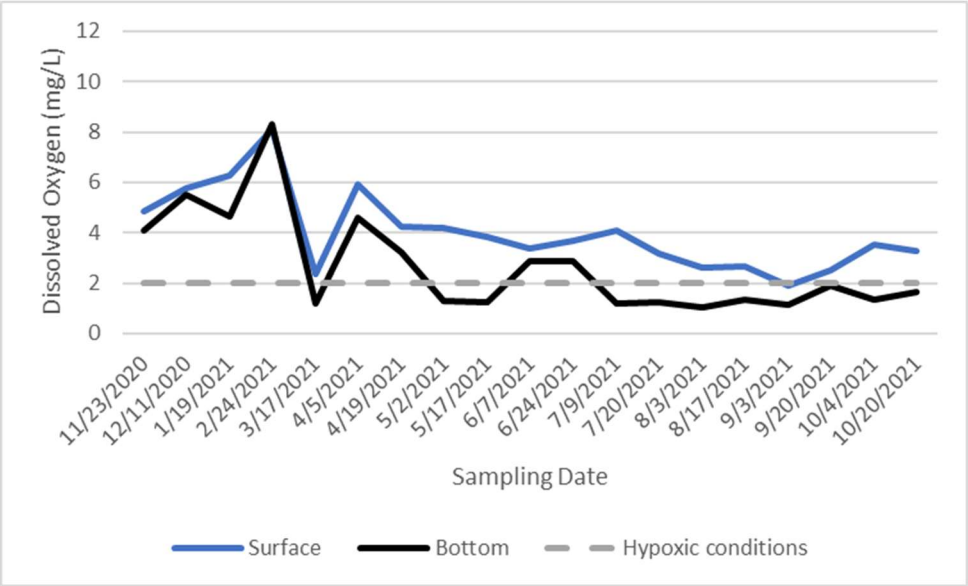

Figure 11: Site 2 surface and bottom dissolved oxygen. Hypoxic conditions when dissolved oxygen < 2mg/L.

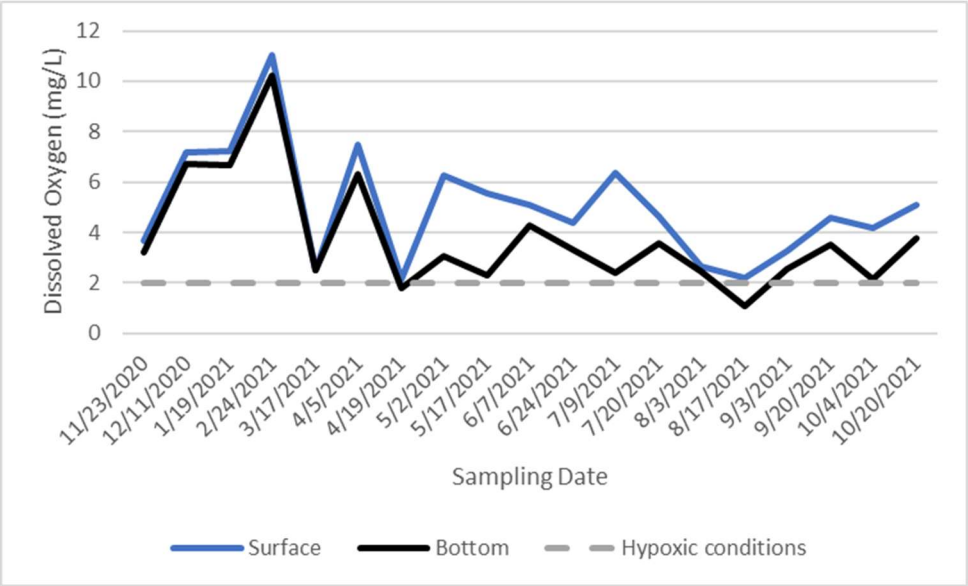

Figure 12: Site 3 surface and bottom dissolved oxygen. Hypoxic conditions when dissolved oxygen < 2mg/L.

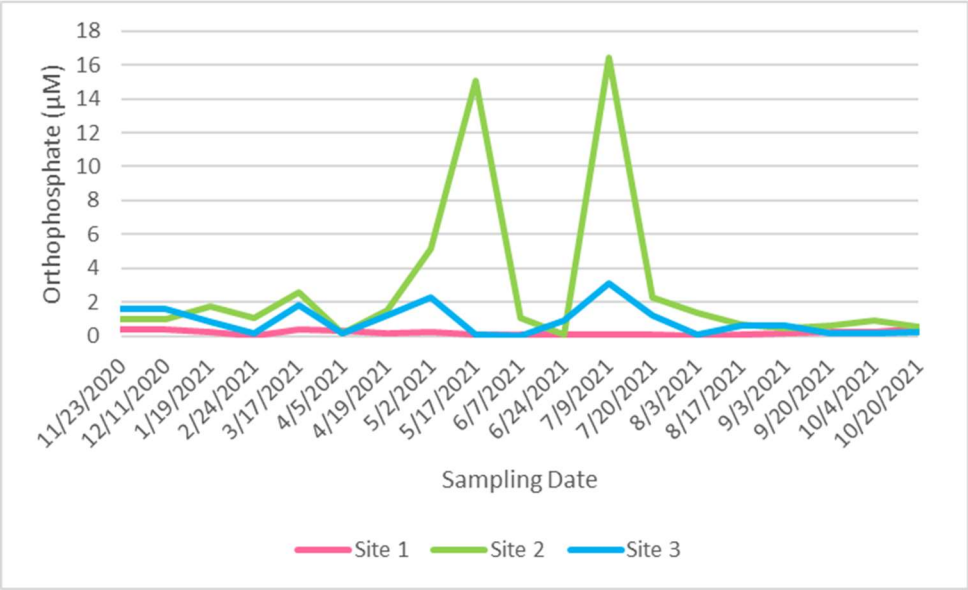

Figure 13: Orthophosphate over time

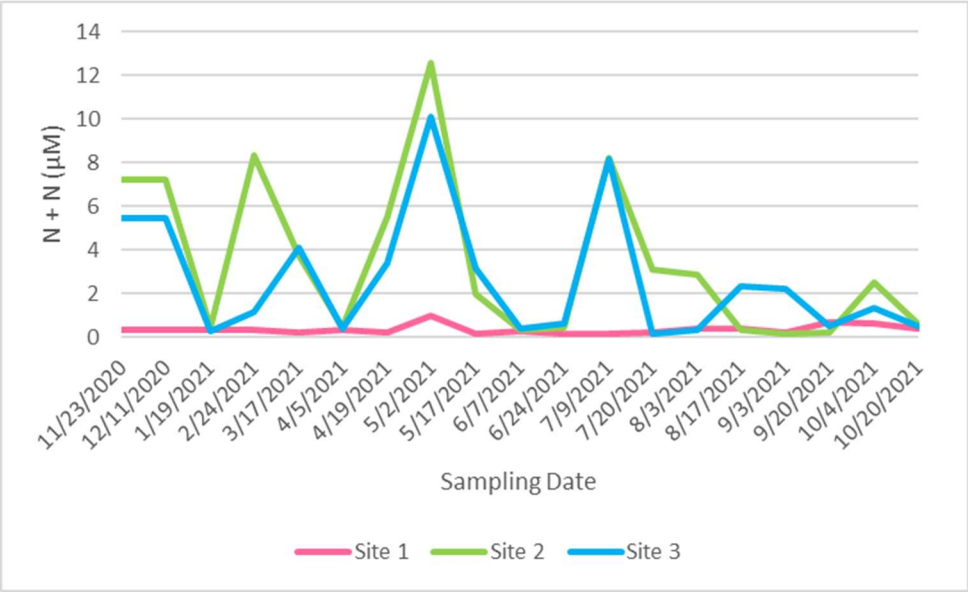

Figure 14: N+N over time

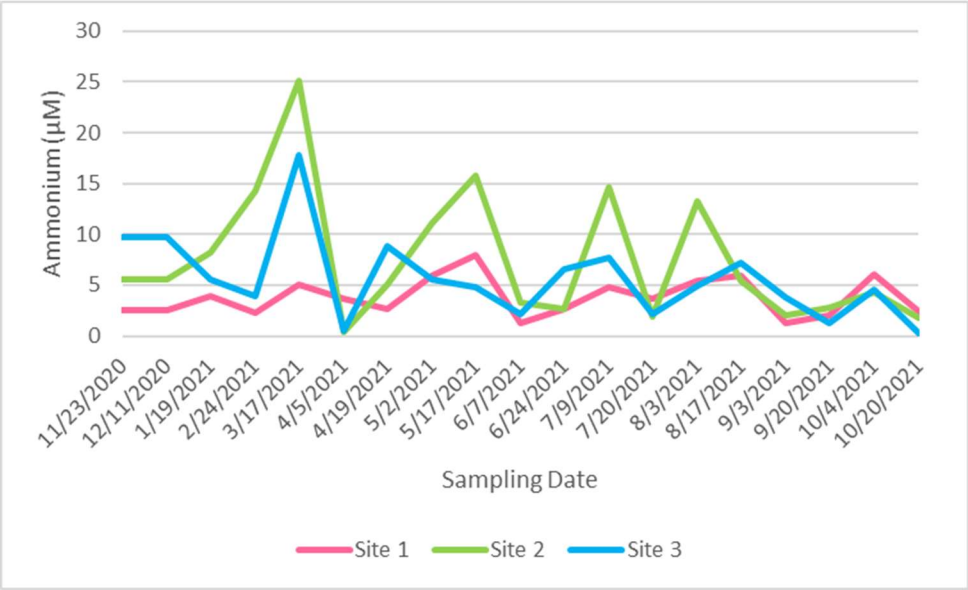

Figure 15: Ammonium over time

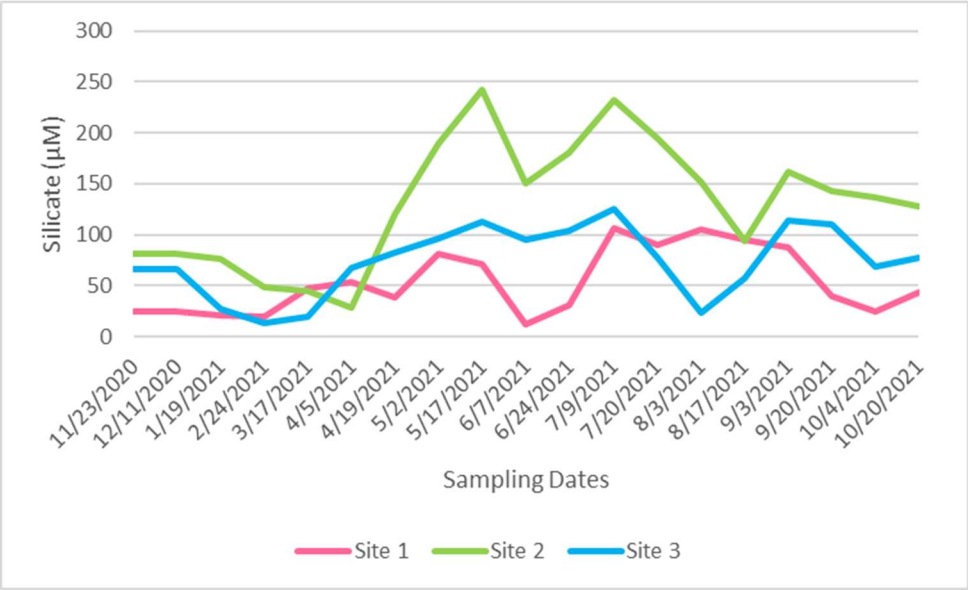

Figure 16: Silicate over time

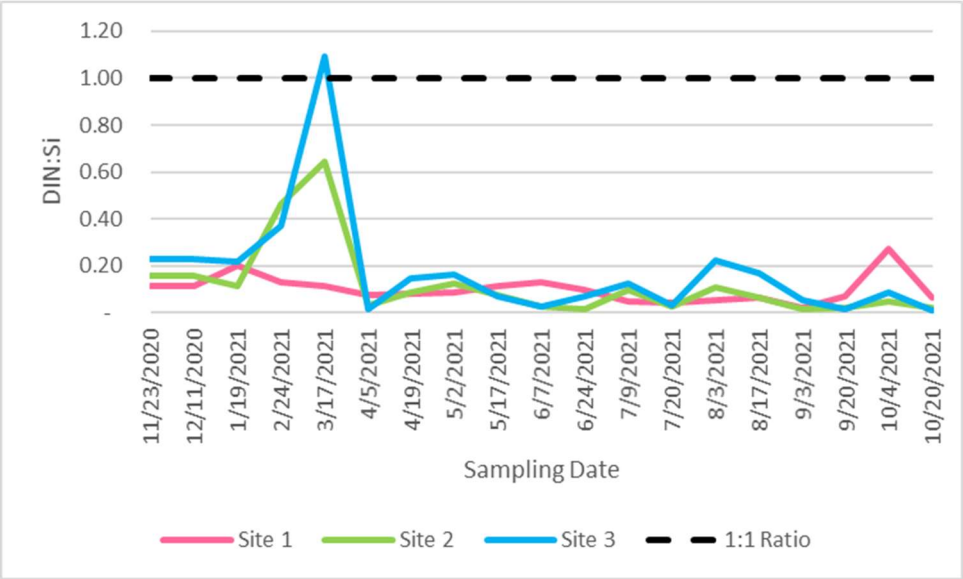

Figure 17: Dissolved inorganic nitrogen: silicate ratios over time. The dashed line indicates a 1:1 ratio. A ratio >1 indicates Si limitation, a ratio <1 indicates N limitation.

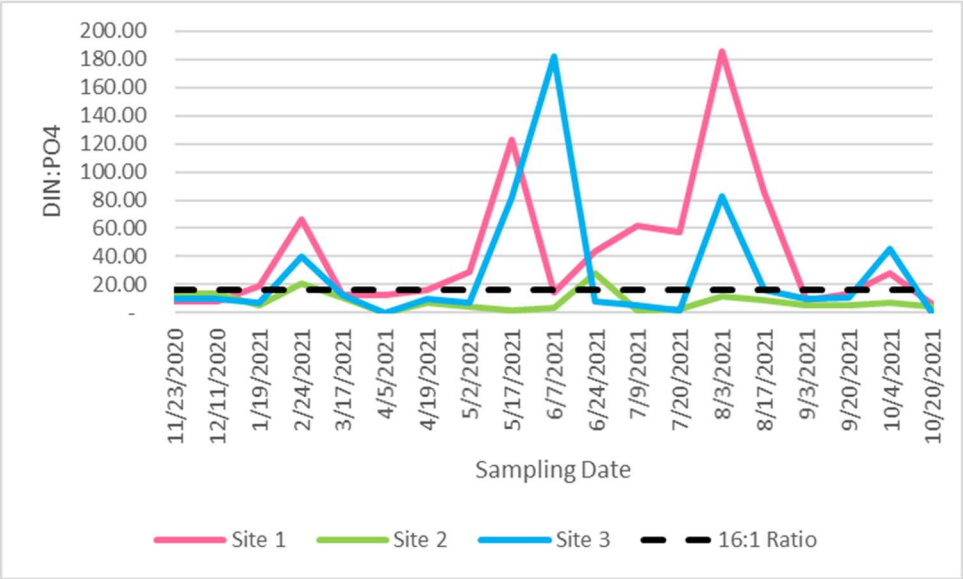

Figure 18: Dissolved inorganic nitrogen: orthophosphate ratios over time. The dashed lined indicate the Redfield Ratio of 16:1. A ratio >1 indicates P-limitation, a ratio <1 indicates N limitation.

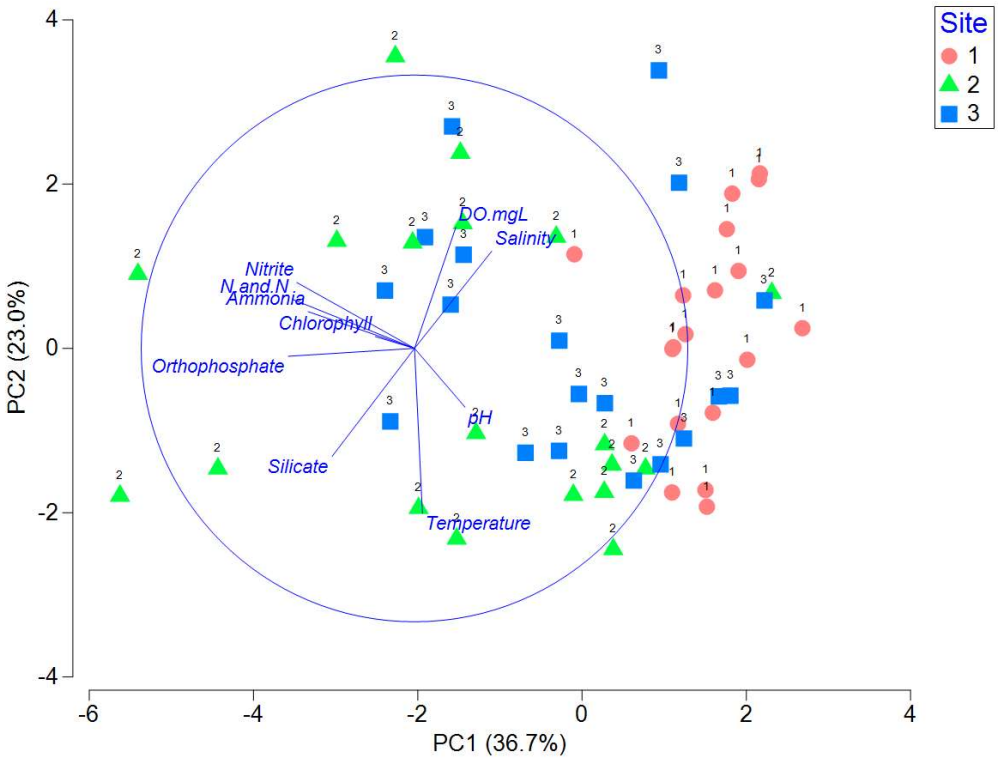

Figure 19: PCA by Site

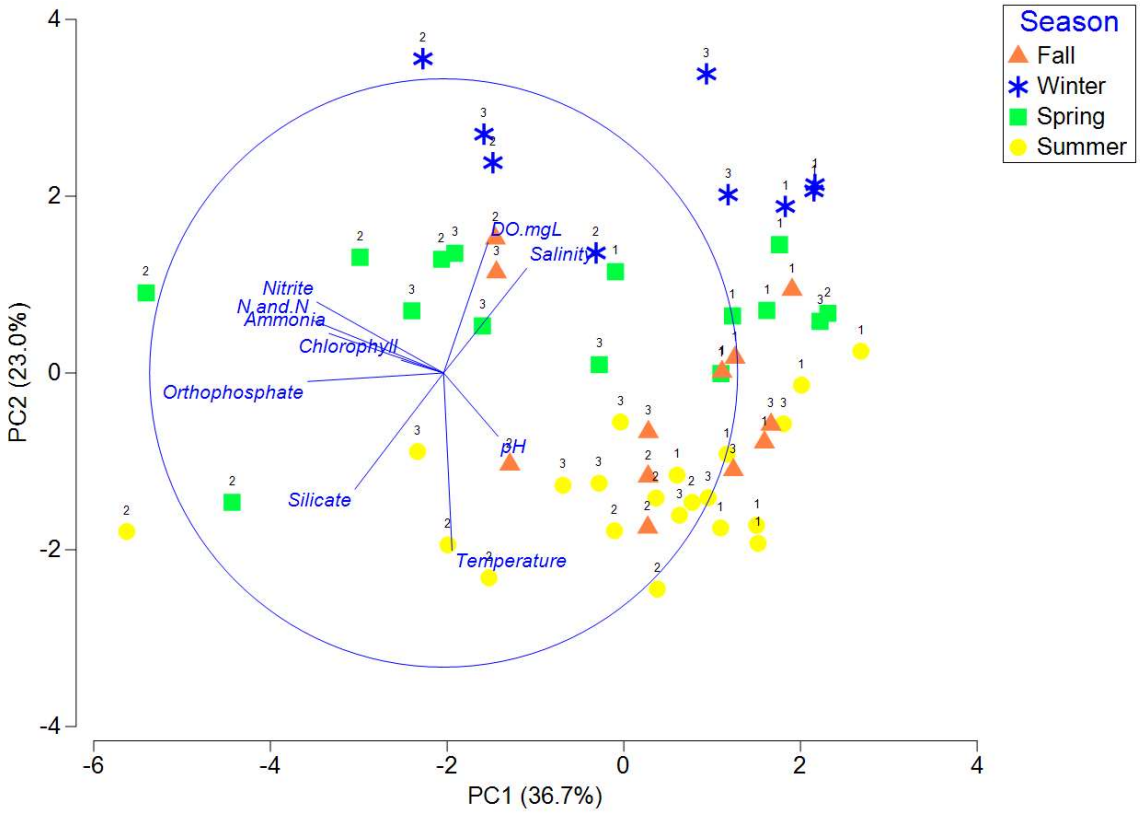

Figure 20: PCA by Season

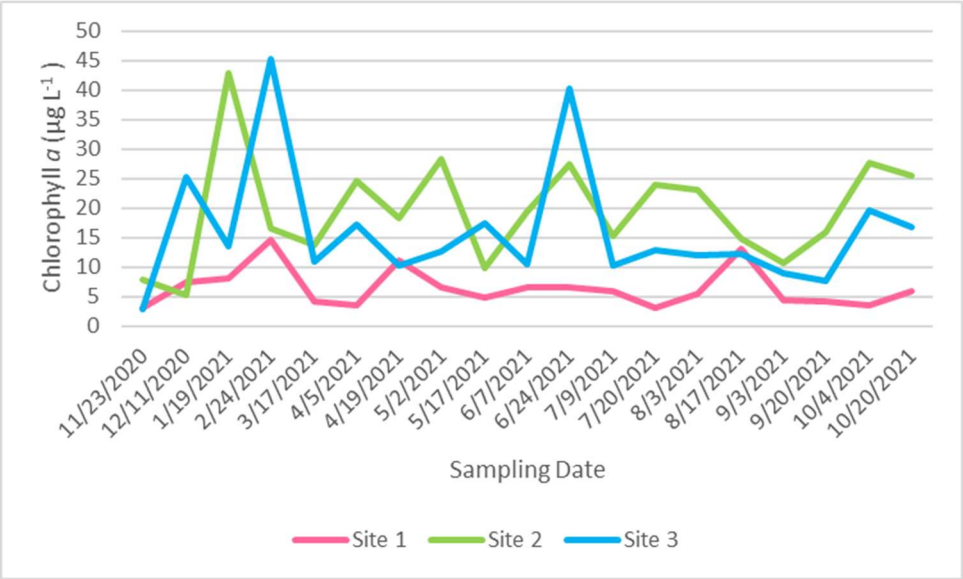

Figure 21: Chlorophyll *a* over time

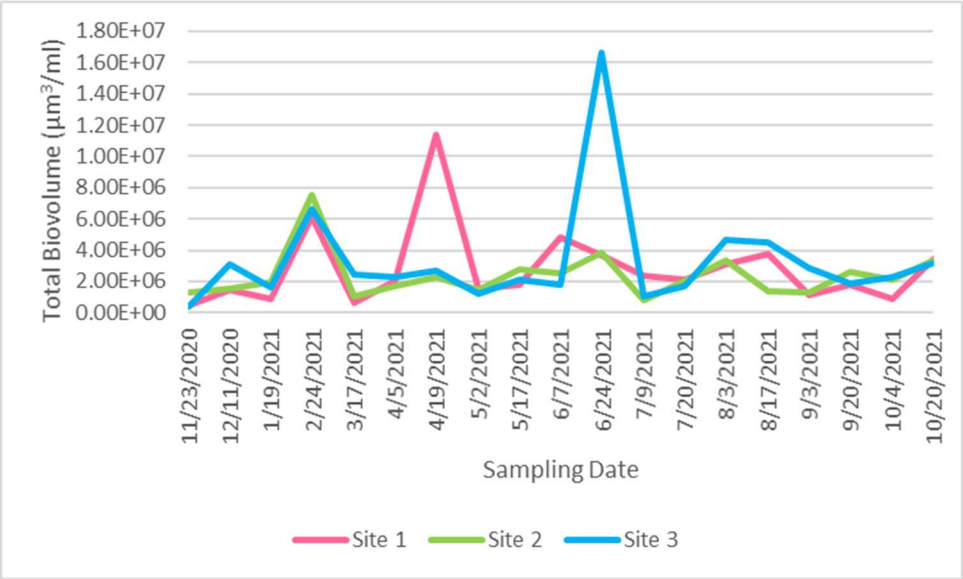

Figure 22: Total biovolume over time

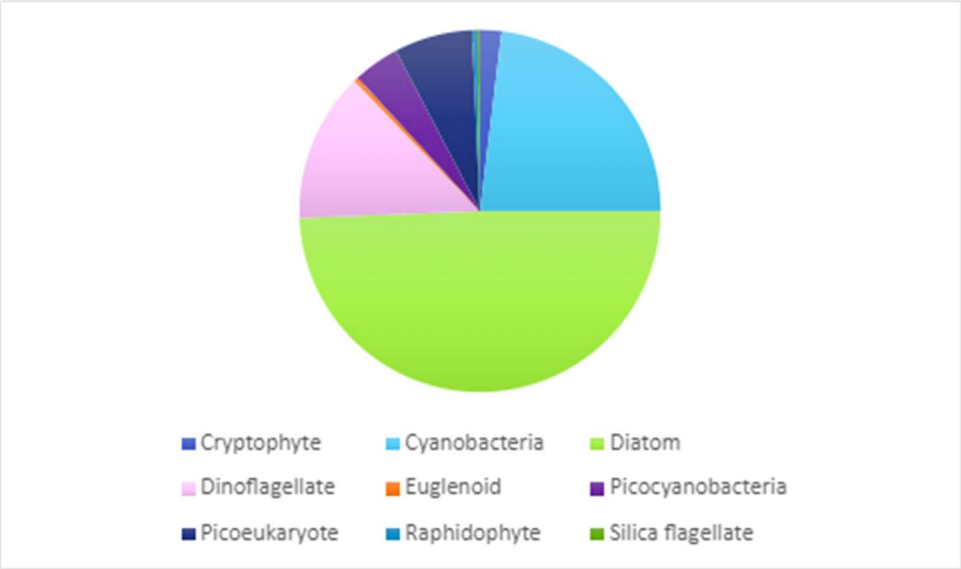

Figure 23: Site 1 average percent contribution to total biovolume by phytoplankton group

Figure 24: Site 2 average percent contribution to total biovolume by phytoplankton group

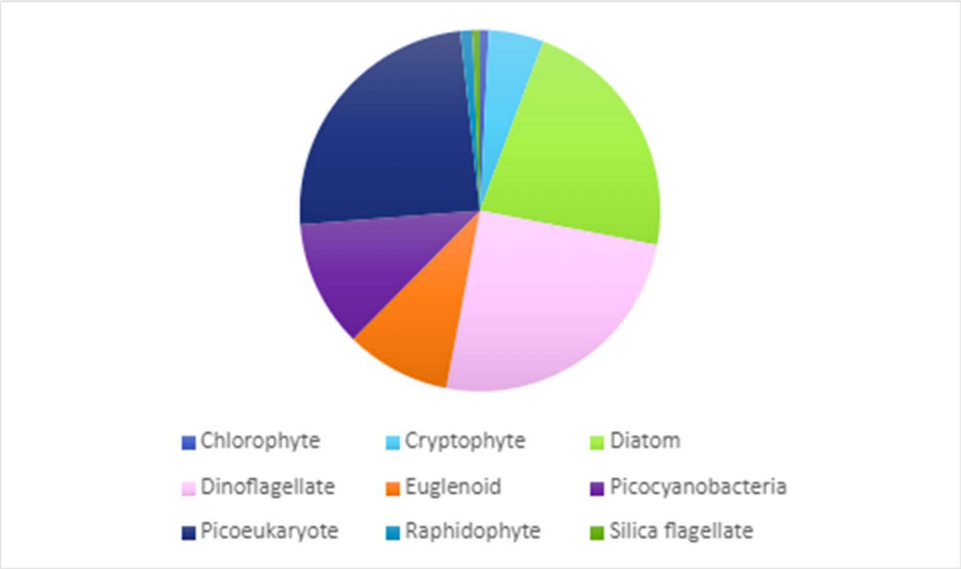

Figure 25: Site 3 average percent contribution to total biovolume by phytoplankton group

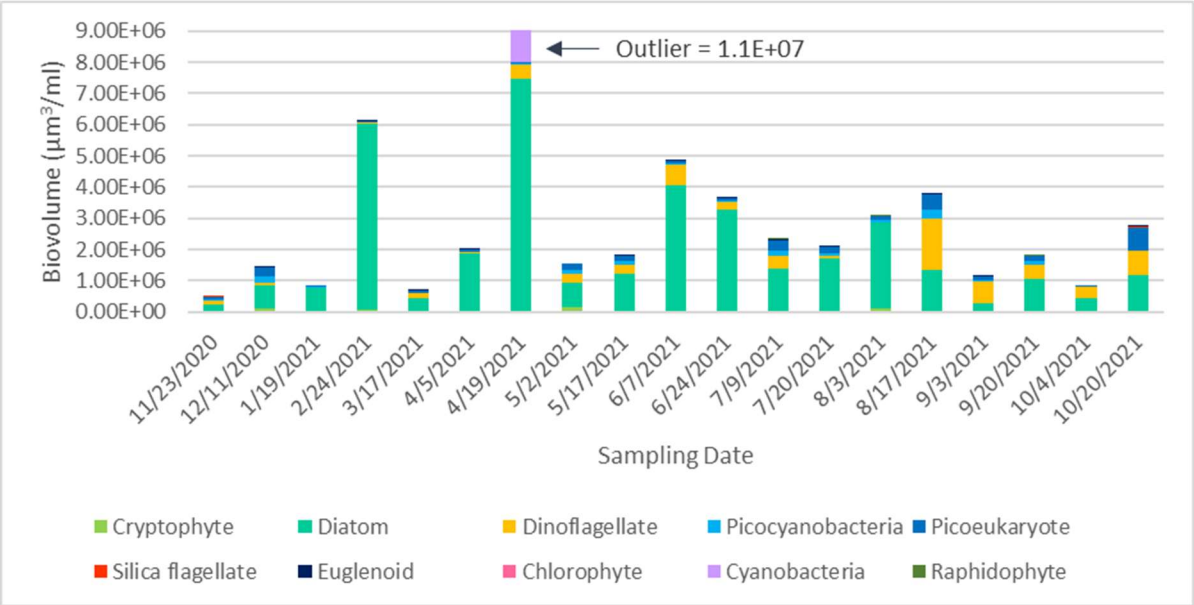

Figure 26: Site 1 total biovolume over time

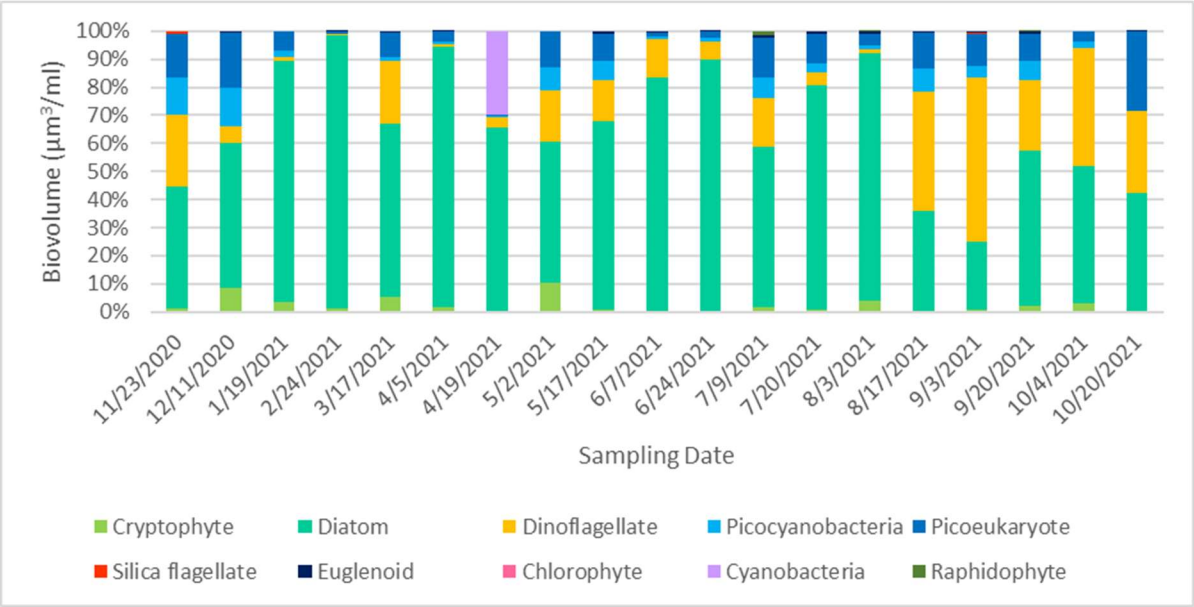

Figure 27: Site 1 phytoplankton group contributions to total biovolume

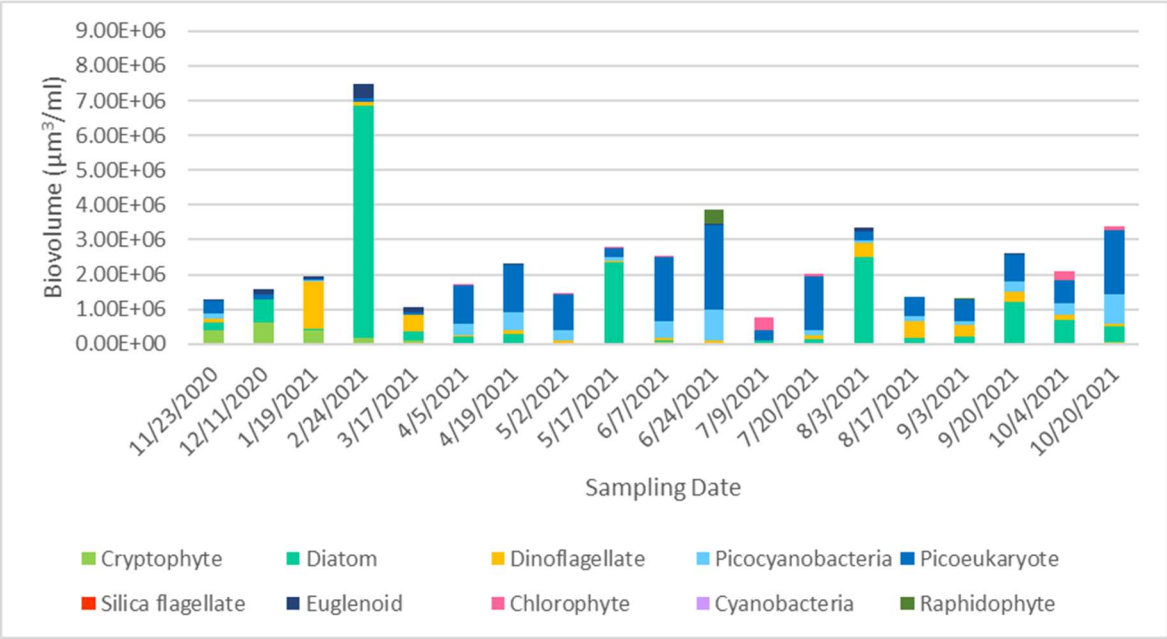

Figure 28: Site 2 total biovolume over time

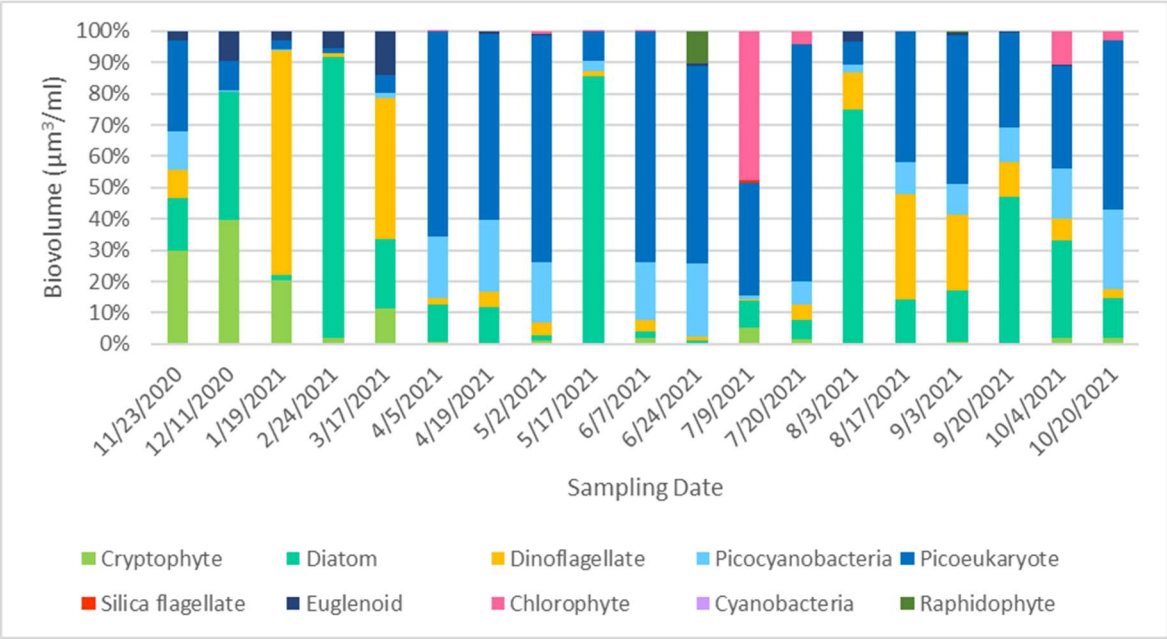

Figure 29: Site 2 phytoplankton group contributions to total biovolume

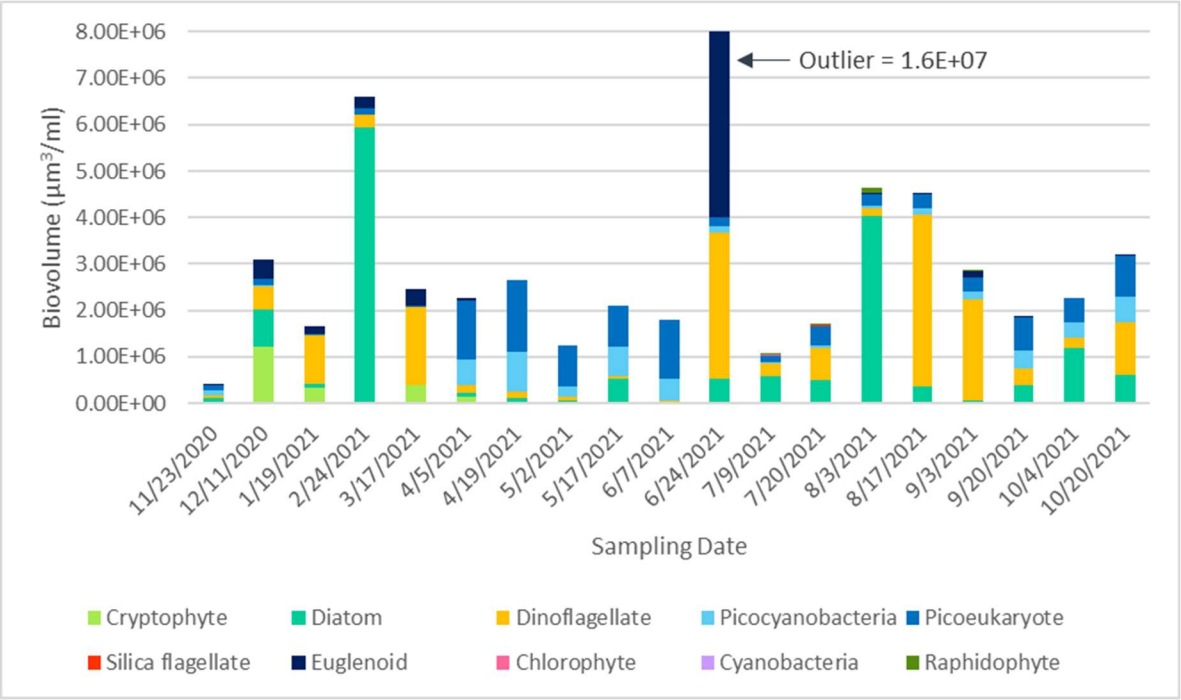

Figure 30: Site 3 total biovolume over time

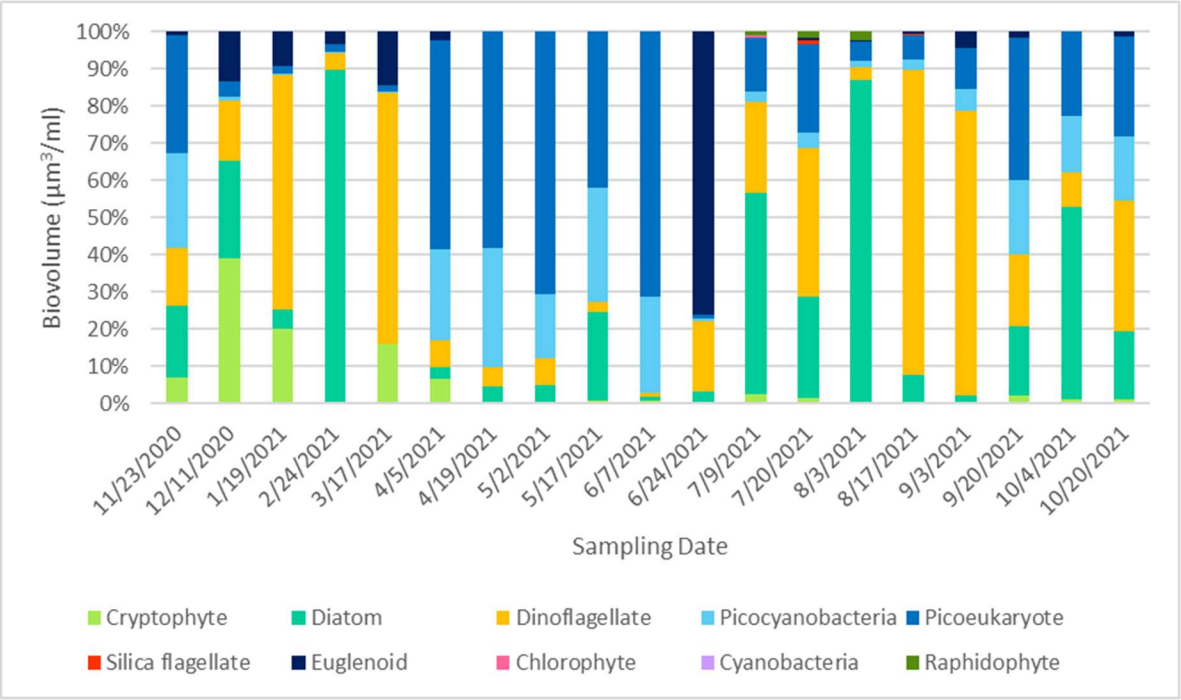

Figure 31: Site 3 phytoplankton group contribution to total biovolume

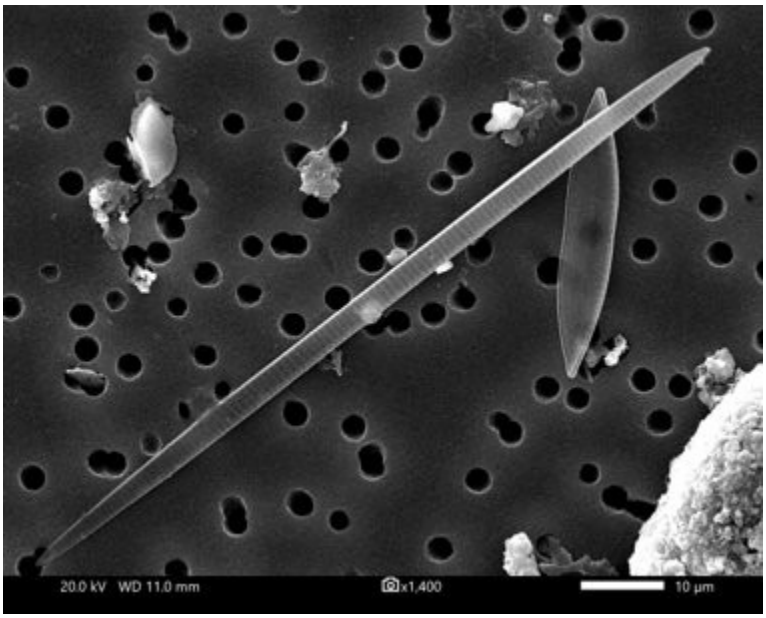

Figure 32: SEM of *pseudonitzschia pungens.*

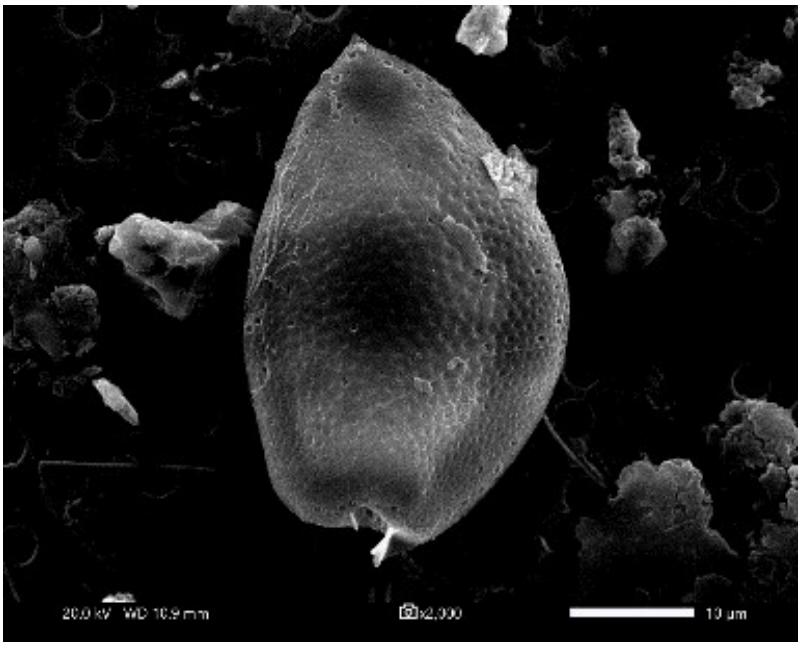

Figure 33: SEM of *Prorocentrum micans*.

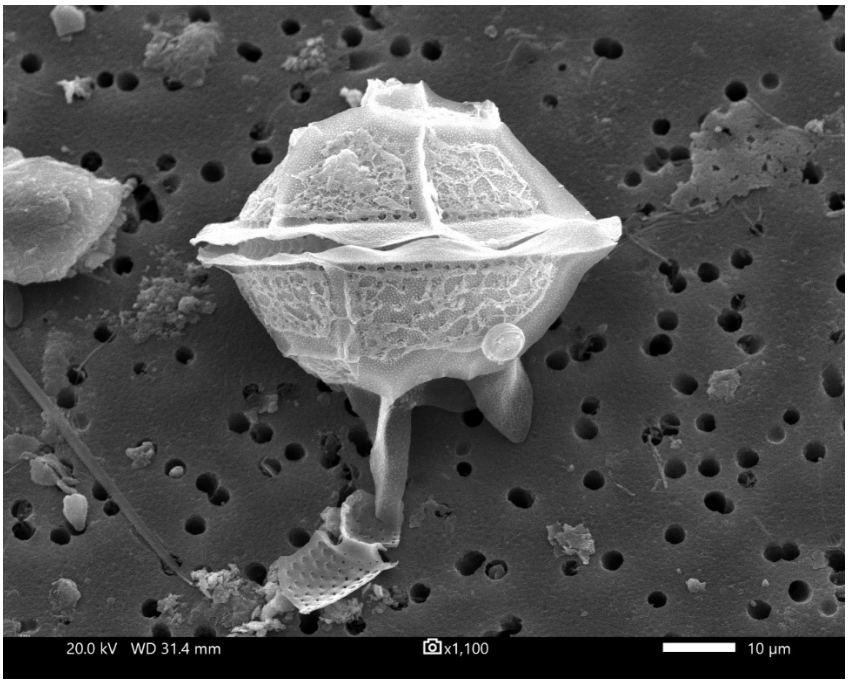

Figure 33: SEM of *Pyrodinium bahamense.*

TABLES

Table 1: Mean ± Standard Deviation of environmental and phytoplankton variables for each site. Different letters (a.b.c) indicate significant differences between sites, as determined by Wilcox post-hoc tests. Variables with the same letter are not significantly different.

Variable	**Site 1**		**Site 2**		**Site 3**	
Ammonium (µM)	3.79 ± 1.86	a	7.52 ± 6.51	a	5.64 ± 4.13	a
Chlorophyll (µg L^{-1})	6.40 ± 3.31	a	19.5 ± 9.02	b	16.1 ± 10.6	b
DO (mg/L)	5.38 ± 1.26	a	4.02 ± 1.57	b	5.03 ± 2.23	a
DO (%)	76.4 ± 14.2	a	56.0 ± 18.1	b	70.9 ± 26.7	a
N+ N (µM)	0.36 ± 0.20	a	3.50 ± 3.65	b	2.64 ± 2.87	b
Orthophosphate (µM)	0.20 ± 0.14	a	2.83 ± 4.70	b	0.877 ± 0.871	b
pH	8.12 ± 0.33	a	7.99 ± 0.285	a	8.15 ± 0.191	a
Salinity	30.4 ± 4.5	a	26.5 ± 8.23	a	29.1 ± 5.99	a
Secchi Depth (m)	0.65 ± 0.19	a	0.68 ± 0.19	a	1.04 ± 0.27	b
Silicate (µM)	53.4 ± 31.8	a	130 ± 61.9	b	73.9 ± 34.0	c
DIN:Si	0.10 ± 0.06	a	0.12 ± 0.16	a	0.18 ± 0.24	a
DIN:PO_4	42.1 ± 47.1	a	8.09 ± 7.17	b	28.4 ± 44.8	a
Temperature (°C)	25.0 ± 4.9	a	25.4 ± 5.04	a	25.7 ± 5.07	a
Total Biovolume (µm^3/ml)	2.8 x 10^6 ± 2.6 x 10^6	a	2.4 x 10^6 ± 1.5 x 10^6	a	3.3 x 10^6 ± 3.5 x 10^6	a
Diatoms (µm^3/ml)	1.9 x 10^6 ± 2.0 x 10^6	a	8.5 x 10^5 ± 1.6 x 10^6	b	8.3 x 10^5 ± 1.5 x 10^6	b
Dinoflagellates (µm^3/ml)	3.5 x 10^5 ± 3.9 x 10^5	a	2.4 x 10^5 ± 3.2 x 10^5	a	8.4 x 10^5 ± 1.1 x 10^6	a
Cryptophytes (µm^3/ml)	4.2 x 10^4 ± 4.6 x 10^4	a	1.0 x 10^5 ± 1.7 x 10^5	a	1.2 x 10^5 ± 2.8 x 10^5	a
Euglenoids (µm^3/ml)	1.4 x 10^4 ± 9.7 x 10^3	a	7.2 x 10^4 ± 1.1 x 10^5	a	1.1 x 10^6 ± 3.5 x 10^6	b
Picoeukaryotes (µm^3/ml)	1.8 x 10^5 ± 1.8 x 10^5	a	8.1 x 10^5 ± 7.1 x 10^5	b	5.3 x 10^5 ± 4.7 x 10^5	b
Picocyanobacteria (µm^3/ml)	1.1 x 10^5 ± 1.5 x 10^5	a	2.5 x 10^5 ± 2.7 x 10^5	a	2.5 x 10^5 ± 2.6 x 10^5	a

Table 2: Correlations between phytoplankton groups and environmental variables. P-values <0.05 are considered statistically significant and are highlighted in yellow.

	Diatom		Dino-flagellate		Pico-eukaryote		Pico-cyano-bacteria		Euglenoid		Chlorophyll *a*		Total Bio-volume	
	rho	p-value	rho	p-value	rho	p-value	rho	p-value	rho	p-value	rho	p-value	rho	p-value
Salinity	-0.09	0.53	-0.06	0.66	-0.21	0.13	-0.06	0.64	0.24	0.13	-0.13	0.34	0.03	0.80
Ammonium (µM)	-0.06	0.66	0.64	0.64	-0.32	0.02	-0.37	< 0.01	0.38	0.01	0.06	0.65	-0.10	0.45
N+N (µM)	-0.31	0.02	-0.12	0.38	0.19	0.16	0.06	0.65	0.35	0.02	0.34	0.01	-0.07	0.58
Ortho-phosphate (µM)	-0.44	< 0.01	0.08	0.56	0.05	0.73	-0.13	0.32	0.16	0.33	0.27	0.04	-0.30	0.02
Silicate (µM)	-0.29	0.03	-0.20	0.14	0.64	< 0.01	0.47	< 0.01	-0.13	0.42	0.31	0.02	-0.05	0.74
DIN:Si	0.11	0.40	0.04	0.75	-0.61	< 0.01	-0.61	< 0.01	0.31	0.05	-0.11	0.41	-0.10	0.47
DIN:PO4	0.47	< 0.01	-0.03	0.79	-0.34	< 0.01	-0.20	0.14	0.13	0.41	-0.34	< 0.01	0.26	0.05
Secchi Depth (m)	-0.22	0.11	0.43	< 0.01	0.05	0.74	0.16	0.25	0.26	0.09	-0.14	0.28	-0.05	0.71
Temperature (°C)	-0.02	0.86	0.20	0.14	0.35	< 0.01	0.33	0.01	-0.14	0.39	-0.06	0.68	0.12	0.37
pH	0.17	0.20	0.05	0.74	0.03	0.82	0.02	0.88	0.09	0.57	0.02	0.87	0.22	0.09
Dissolved Oxygen (mg/L)	0.29	0.03	-0.19	0.17	-0.34	0.01	-0.33	0.01	0.15	0.34	-0.06	0.68	-0.004	0.98
Precipitation (inches)	0.17	0.47	0.30	0.20	0.14	0.57	0.23	0.34	0.17	0.57	-0.17	0.49	0.19	0.45